

## ONLINE-ONLY DATA SUPPLEMENT

### EXPANDED METHODS

#### Generation of cardiac-specific CX43/PKP2 knockout mice

A C57BL/6 CX43<sup>flox</sup> mice line<sup>1</sup> was purchased from The Jackson Laboratory (B6.129S7-Gja1<sup>tm1.1Dtg/J</sup>, stock number 008039). The CX43 flox/flox mice possess loxP sites flanking exon 2 of the GJA1 gene, and these mice were bred with PKP2flox/flox/ $\alpha$ MHC-Cre-ER(T2) mice to obtain the mice with (CX43flox/flox)/(PKP2flox/flox)/Cre+, and the CX43flox/wt)/(PKP2flox/flox)/Cre+ mice. Generation of the PKP2flox/flox/Cre+ mice has been described previously<sup>2</sup>. The  $\alpha$ MHC-Cre-ER(T2) mice contain the  $\alpha$  myosin heavy chain promoter and the ligand binding domain of the human estrogen receptor<sup>3,4</sup>. The resulting CX43/PKP2flox/flox/cre+ mice developed normally without functional or structural deficits. The genotypes of CX43flox mice were identified by PCR reaction with the loxP primers (forward CTTTGACTCTGATTACAGAGCTTAA and reverse GTCTCACTGTTACTTAACAGCTTGA). For  $\alpha$ MHC-Cre-ER(T2) genotyping the forward primer TTATGGTACCACATAGACCTCTGACA and reverse TGCTGTTGGATGGTCTTCACAG were used. All procedures conformed to the Guide for Care and Use of Laboratory Animals published by the US National Institutes of Health and were approved by the NYU IACUC committee under protocol number 160726-03. Mice were intraperitoneally injected 4 consecutive days with tamoxifen (3 mg dissolved in sterile peanut oil with 10% ethanol; giving an approximate tamoxifen dose of 0.1 mg/g body weight). Binding of tamoxifen to the estrogen receptor induced the cardiomyocyte specific Cre-mediated deletion of the CX43 and PKP2 genes. All experiments were performed in C57BL/6 CX43/PKP2-cKO mice and Cre-negative, tamoxifen treated, littermates were used as controls. Both genders were included and all animals were between 3 and 6 months of age.

#### RNASeq analysis

Five control and 4 PKP2-cKO mice were euthanized 14 days post-TAM; the hearts were harvested, the free wall of the RV and the LV were dissected and processed separately for RNA extraction (RNA-easy Mini kit; Qiagen). mRNA-Seq library preps were made using the Illumina TruSeq® RNA Library Preparation Kit v2 using 500 ng of total RNA as input, amplified by 12 cycles of PCR, and run on an Illumina 2500 (v4 chemistry), as single read 50 at the Genome Technology Center at NYU Langone Health. Approximately 200 million reads per sample were generated. Sequencing results were demultiplexed and converted to FASTQ format using Illumina

Bcl2FastQ software. Quality Control (QC) for the RNA-Seq reads was assessed using FastQC software. Next, reads were aligned to the mouse genome (build mm10/GRCm38) with Spliced Transcripts Alignment to a Reference (STAR<sup>5</sup>). PCR duplicates were removed using the Picard toolkit (open-source, MIT license). HTSeq package was utilized to generate counts for each gene. The read counts of each transcript were normalized to the length of the individual transcript and to the total mapped read counts in each sample and expressed in counts per millions (CPM)<sup>5</sup>. In order to examine if groups clustered separately from one another we first performed a Principal Component Analysis (PCA). PCA is based on two principal components PC1 and PC2<sup>6</sup>. The first principal component (PC1) is the direction along which the samples show the largest variation. The second principal component (PC2) is the direction uncorrelated to the first component along which the samples show the largest variation. Next, we visualized the genes with a largest variance using a hierarchical clustering heatmap. For each gene, we compared the expression levels between left ventricle and right ventricle RNAs for Control and PKP2-cKO samples. Gene expression differences were evaluated by paired *t*-tests corrected via the Benjamini and Hochberg method. We used the DESeq2 package for data analysis (<https://bioconductor.org/packages/release/bioc/html/DESeq2.html>).

### **Cardiomyocyte dissociation.**

Murine ventricular myocytes were obtained by enzymatic dissociation. Mice were injected with 0.1 mL heparin (500 IU/mL i.p.) 20 min before heart excision and anaesthetized by inhalation of 100% CO<sub>2</sub>. Deep anesthesia was confirmed by lack of response to otherwise painful stimuli. The mouse was then euthanized and the heart surgically removed via thoracotomy and placed in a Langendorff column. The isolated hearts were perfused sequentially at a constant flow rate of 3 mL/min with Ca<sup>2+</sup>-free solution containing (in mM): 113 NaCl, 4.7 KCl, 1.2 MgSO<sub>4</sub>, 0.6 Na<sub>2</sub>HPO<sub>4</sub>, 0.6 KH<sub>2</sub>PO<sub>4</sub>, 12 NaHCO<sub>3</sub>, 10 KHCO<sub>3</sub>, 10 HEPES, 5.5 Glucose and 30 Taurine, pH 7.40 with NaOH and then an enzyme (collagenase type II; Worthington, Lakewood, NJ, USA) solution for 10 min. Perfusate temperature was maintained at 37°C. After digestion, the left ventricular free wall and the right ventricular free wall tissues were separated, cut into small pieces, and minced by gentle mechanical agitation with a Pasteur pipette. The isolated cardiomyocytes were suspended in 10 mL of stop buffer (Ca<sup>2+</sup>-free perfusion buffer with 5% bovine calf serum) and the Ca<sup>2+</sup> concentration was increased gradually to 1.0 mM. Cardiomyocytes were kept in Tyrode's solution containing (in mM): 148 NaCl, 5.4 KCl, 1.0 MgCl<sub>2</sub>, 1.0 CaCl<sub>2</sub>, 0.4 NaH<sub>2</sub>PO<sub>4</sub>, 15 HEPES and 5.5 Glucose, pH 7.40. Cells were used within 8 h after isolation.

## Ca<sup>2+</sup> imaging in single ventricular myocytes.

### *Ca<sup>2+</sup> transients and Ca<sup>2+</sup> sparks*

Isolated ventricular myocytes were loaded for 10 min with Fluo-8 AM (AAT Bioquest) in Tyrode's solution containing (in mM): 140 NaCl, 4 KCl, 1.8 CaCl<sub>2</sub>, 1 MgCl<sub>2</sub>, 10 HEPES and 5.6 glucose followed by additional 10 min wash in Tyrode's solution. The Ca<sup>2+</sup> transients were induced by applying depolarizing pulses at 1 Hz using a pair of electrodes coupled to a stimulator (MyoPacer, IonOptix). Ca<sup>2+</sup> fluorescence was imaged using a laser scanning confocal microscopy system (Leica TCS SP5) fitted with a 63x oil immersion objective lens. Dyes were excited at 488 nm using an Ar laser and fluorescence emission at wavelengths >510 nm was detected. To measure Ca<sup>2+</sup> transients or Ca<sup>2+</sup> sparks, line-scan images were captured at 1.43 ms/line with LAS AF (Leica) software. Recording of Ca<sup>2+</sup> sparks was preceded by a train of electrical pulses at 1 Hz for 10 sec. Under this condition, the frequency of Ca<sup>2+</sup> sparks was stable during the experimental period. To quantify Ca<sup>2+</sup> transients, local averaged Ca<sup>2+</sup> signals were measured using ImageJ (NIH) software. Traces of local Ca<sup>2+</sup> transients were expressed as the mean fluorescence of each line normalized to the mean resting fluorescence (F/F<sub>0</sub>). For automated detection and analysis of Ca<sup>2+</sup> sparks in linescan images, we used a thresholding algorithm, the SparkMaster plugin, implemented within ImageJ software<sup>6</sup>.

### *Determination of [Ca<sup>2+</sup>]<sub>i</sub>*

For ratiometric Ca<sup>2+</sup> imaging to determine quantitatively [Ca<sup>2+</sup>]<sub>i</sub>, isolated ventricular myocytes were loaded with 3 μM Fura Red AM for 30 min and the dye was alternately excited with the 458 and 488 nm argon laser. Fluorescence emission at wavelengths >585 nm was detected using a laser scanning confocal microscopy system (Leica TCS SP5). The paired images were analyzed by the method described by Lohr et al<sup>7</sup>. Briefly, a Fura Red fluorescence ratio (F<sub>458</sub>/F<sub>488</sub> or R<sub>458/488</sub>) was calculated from the fluorescence intensity emitted under each excitation wavelength. The analysis utilized the LAS X (Leica) software and the R<sub>458/488</sub> images were obtained with ImageJ plugin Ratio Plus. The R<sub>458/488</sub> was calibrated to the [Ca<sup>2+</sup>]<sub>i</sub> using the formula described by Grynkiewicz et al.<sup>8</sup>

$$[\text{Ca}^{2+}]_i = K_d \frac{Sf_2 R - R_{\min}}{Sb_2 R_{\max} - R}$$

where  $K_d$  is the dissociation constant (140 nM; Thermo Fisher) and  $R$  is the fluorescence ratio.  $Sf_2$  and  $Sb_2$  are the fluorescence intensities of Ca<sup>2+</sup>-free and Ca<sup>2+</sup>-bound dyes excited at 488 nm, respectively.  $R_{\min}$  and  $Sf_2$  were determined in a Ca<sup>2+</sup>-free solution containing 1 mM EGTA, and  $R_{\max}$  and  $Sb_2$  were determined in a solution containing 2 mM Ca<sup>2+</sup>.  $R_{\min}$ ,  $R_{\max}$ ,  $Sf_2$  and  $Sb_2$  were

determined experimentally using cells that were permeabilized with 20  $\mu\text{M}$  of the  $\text{Ca}^{2+}$  ionophore 4-bromo-A23187 (Sigma-Aldrich) and 50  $\mu\text{M}$  ionomycin (EMD Millipore) to allow  $[\text{Ca}^{2+}]_i$  to equilibrate with  $[\text{Ca}^{2+}]_o$ .

#### *SR $\text{Ca}^{2+}$ load in permeabilized myocytes*

To measure SR  $\text{Ca}^{2+}$  load in permeabilized myocytes, cells were plated on glass-bottom dishes coated with 1 mg/mL laminin and maintained in bath solution containing (in mM) 135 NaCl, 4 KCl, 1.8  $\text{CaCl}_2$ , 1  $\text{MgCl}_2$ , 10 HEPES, 1.2  $\text{NaH}_2\text{PO}_4$ , and 10 glucose, pH 7.40, until used. Myocytes were permeabilized with 50  $\mu\text{g}/\text{mL}$  saponin in 10 nM free  $[\text{Ca}^{2+}]$  'internal' solution, containing (in mM) 0.5 EGTA, 10 HEPES, 120 K-aspartate, 0.56  $\text{MgCl}_2$ , 5 Mg-ATP, 10 reduced glutathione, 5 phosphocreatine, 5 U/mL creatine phosphokinase, 8% dextran (Mr: 40,000), pH 7.20, and enough  $\text{CaCl}_2$  to adjust free  $[\text{Ca}^{2+}]$  (MaxChelator). Subsequently, permeabilized myocytes were perfused with 70 nM free  $[\text{Ca}^{2+}]$  internal solution supplemented with 25  $\mu\text{M}$  Fluo-4 pentapotassium salt (Thermo Fisher). Line-scan images were acquired at the sampling rate of 1.43 ms/line, using Leica TCS SP5 confocal microscope with a 63x oil immersion objective lens. After 10 s of applying a train of electrical pulses at 1 Hz, 10 mM caffeine was rapidly applied. Under this condition, SR  $\text{Ca}^{2+}$  content was stable during the experimental period.

#### *Equating SR load in PKP2cKO-RV myocytes by changing $[\text{Ca}^{2+}]_o$ ; effect of PKC inhibitors*

A specific set of experiments was designed to measure  $\text{Ca}^{2+}$  spark frequency in non-permeabilized PKP2cKO-RV myocytes under conditions of equal SR load (see below for ratiometric method of  $\text{Ca}^{2+}$  detection). For this purpose,  $[\text{Ca}^{2+}]_o$  was lowered from the control value of 1.8 mM to 0.6 mM, a 10 mM caffeine pulse was applied, and SR re-loaded using a train of field stimulation (1 Hz for 10 seconds). A specific set of experiments showed that PKP2cKO-RV SR load at this lower  $[\text{Ca}^{2+}]_o$  matched that recorded from control myocytes and from PKP2cKO-LV cells. Under these conditions, spark frequency, and its sensitivity to two different PKC inhibitors (GF109203X; 1  $\mu\text{M}$ ; 5 min) or calphostin C (0.2  $\mu\text{M}$ ; 5 min) was examined using the protocol for spark frequency described above.

#### *Detection of $\text{Ca}^{2+}$ by a two-dye ratiometric method.*

Additional experiments (specified in the "Results" section in the main manuscript) for detection of SR load and diastolic  $[\text{Ca}^{2+}]$  in non-permeabilized myocytes relied on the use of a ratiometric method as described in<sup>9,10</sup>. Briefly, myocytes were loaded with the  $\text{Ca}^{2+}$ -sensitive dyes Fluo-3 AM (1.67  $\mu\text{M}$ ) and Fura Red AM (5  $\mu\text{M}$ ; Molecular Probes) for 30 min. The excitation wavelength was

488 nm. Fluo-3 (emission at 505–550 nm) and Fura Red (emission at >615 nm) were imaged simultaneously. To measure diastolic  $[Ca^{2+}]$ , cells were imaged in a 2-D scanning mode at the sampling rate of 10.24 s/frame with 1,024×1,024 pixels resolution. SR  $Ca^{2+}$  load was measured in line-scanning mode at the sampling rate of 1.43 ms/line. When the cells were exposed to 10 mM caffeine, the fluorescence from Fluo-3 was increased, while the fluorescence of Fura Red was reduced. In both experiments, images were recorded after 10 s of rest following a train of electrical pulses at 1 Hz, using Leica TCS SP5 confocal microscope with a 63x oil immersion objective lens. The ratio of the intensity of the two images ( $F_{Fluo-3}/F_{Fura\ Red}$ ) was calculated by using LAS X software and the  $F_{Fluo-3}/F_{Fura\ Red}$  images were obtained with ImageJ plugin Ratio Plus.

#### *Mitochondrial $Ca^{2+}$ dynamics*

Ventricular myocytes were loaded with 2  $\mu$ M Rhod-2 AM (Thermo Fisher) at 4°C for 70 min. At 4°C, the cytosolic esterase activity is sufficiently low that the AM esters can reach the mitochondria before being hydrolyzed<sup>11</sup>. Cold loading was followed by warm incubation (37°C, 5 h). During warm incubation, the dye molecules in the cytosol gradually leak out to the extracellular space<sup>11</sup>. Some cells were further incubated with 200 nM MitoTracker Deep Red FM (Thermo Fisher) for 10 min at 37°C. After washing twice, the cells were placed on the stage of a Leica TCS SP5 confocal microscope (63x oil immersion lens) where Rhod-2 fluorescence was recorded by excitation at 543 nm and measurement of the emitted light at 560-600 nm. MitoTracker was excited at 633 nm and fluorescence emission at 650-800 nm was detected. Images were acquired with LAS AF software. Image analysis and quantification was made using LAS X and ImageJ software. After this protocol, we observed patterns of Rhod-2 loading similar to that of MitoTracker staining, suggesting that Rhod-2 was selectively loaded into Mitochondria. To evaluate the mitochondrial  $Ca^{2+}$  dynamics in response to electrical stimulation, we monitored Rhod-2 fluorescence signal immediately before ( $F_0$ ) and after (F) stimulation at 3 Hz pacing frequency for 1 min.

#### **Mass spectrometry measurements of RyR2 phosphorylation**

Tissue homogenates were prepared from four hearts from Control and PKP2cKO mice 14 days post-TAM. The free wall of the LV and the RV were dissected out and immediately snap frozen. Tissue homogenates were prepared as previously described<sup>12</sup>. In brief, free wall tissue of each mice was homogenized separately using Precellys 24 (Bertin Instruments) in an ice-cold lysis buffer supplemented with 1% Triton X-100, protease and phosphatase inhibitors and allowed to solubilize for 2h at 4°C. Subsequently, lysates were centrifuged to remove debris and the protein

concentrations were determined using Quick Start Bradford Dye Reagent (Bio-rad). Immunoprecipitations were performed by pre-clearing 1.5mg of lysate using Dynabeads Protein G (Thermo Fisher). The pre-cleared lysate was incubated with 2µg anti-RyR2 (ARR-002, Alomone) overnight at 4°C. The complex was captured using Dynabeads Protein G, washed with lysis buffer and eluted in 1X SDS loading dye supplemented with 100 mM DTT by heating it at 70°C for 10min. The precipitate was run on SDS-PAGE, and the part corresponding to the molecular weight of RyR2 was excised. The proteins were in-gel digested with trypsin, as previously described<sup>13</sup>. Briefly, excised gel bands from Coomassie stained SDS-PAGE separated proteins were minced, destained, reduced and alkylated. The proteins were extracted and digested with sequencing grade trypsin (Promega) overnight at 37°C. The activity of trypsin was subsequently quenched by TFA acidification and the resulting peptides were extracted by acetonitrile/water and desalted and concentrated on C<sub>18</sub> STAGE tips. Peptides were eluted with 2x20ul 40% ACN, 0.5% AcOH and the organic solvents were removed in a vacuum centrifuge. Peptide samples were analyzed by online reversed-phase liquid chromatography coupled to a Q-Exactive HF-X quadrupole Orbitrap tandem mass spectrometer (LC-MS/MS, Thermo Electron, Bremen, Germany). Peptide samples were diluted in 5%ACN, 0.1% TFA in 96-well microtiter plates and autosampled (2ul injection volume) into a nanoflow Easy-nLC system (Proxeon Biosystems, Odense, Denmark). Peptide samples were separated on 15cm fused-silica emitter columns pulled and packed in-house with reversed-phase ReproSil-Pur C18-AQ 1.9µm resin (Dr. Maisch GmbH, Ammerbuch-Entringen, Germany) in a 30min multi-step linear gradient (Buffer A: 0.1% formic acid, Buffer B: 0.1% formic acid, 80% ACN; 10-30% Buffer B in 25min, 30-45% Buffer B in 5min, 45-80% Buffer B in 30s). Column effluent was directly ionized in a nano-electrospray ionization source operated in positive ionization mode and electrosprayed into the mass spectrometer. Full-MS spectra (350-1400 m/z) were acquired after accumulation of 3,000,000 ions in the Orbitrap (maximum fill time of 45ms) at 60,000 resolution. A data-dependent Top12 method then sequentially isolated the most intense precursor ions (up to 12 per full scan) for higher-energy collisional dissociation (HCD) in an octopole collision cell. MS/MS spectra of fragment ions were recorded at resolution of 15000 after accumulation of 100,000 ions in the Orbitrap (maximum fill time of 22ms). Raw MS data was processed using the MaxQuant software (Max-Planck Institute of Biochemistry, Department of Proteomics and Signal Transduction, Munich) and proteins identified with the built-in Andromeda search engine by searching MS/MS spectra against an in-silico tryptic digest of a database containing all reviewed SwissProt mouse protein entries. The MS/MS spectra were searched with Carbamidomethyl-Cysteine as fixed modification, as well as oxidation (M), acetylation of protein N-termini and Gln->pyro-Glu and phospho(STY) as variable modifications. A maximum of two

missed cleavages and six variable modifications was allowed. The minimum peptide length was set to 7 amino acids (default) and minimum Andromeda score required for modified peptides was 25, with minimum delta score of 6 (default). First search tolerance was 20ppm (default) and main search tolerance was 4.5ppm (default), requiring strict specificity of tryptic peptides. Due to the similarity of the samples the match-between-runs option was enabled with default parameters. False-discovery rate cutoffs were set to 1% on peptide, protein and site decoy level (default), only allowing high-quality identifications to pass. All peptides were used for protein quantification. Protein identification results were further processed using the Perseus software suite.

### **Western blot analysis**

To analyze expression levels of PKP2, total Cx43 and phosphoCx43-S368, we used a standard protocol<sup>2</sup>. Briefly PKP2cKO and control mice were euthanized (CO<sub>2</sub> inhalation 2% for 5 – 10 min, confirmed by cervical dislocation) at 14 days post-TAM. The mice ventricular samples were cryopreserved immediately in liquid nitrogen. Ventricular samples were then homogenized in extraction buffer containing protease and phosphatase inhibitors (50 mM Tris pH 8.0, 150 mM NaCl, 0.02% Sodium azide, 1% Triton X-100, 1 mM PMSF, 1 mM Na<sub>3</sub>VO<sub>4</sub>, 50 mM NaF and Complete Protease Inhibitor (Roche)). Protein concentration was determined using the BCA kit (Thermo Fisher). Samples were run on 4-12% precast polyacrylamide SDS gradient gels (BioRad) and transferred onto nitrocellulose membranes (BioRad), subsequently incubated in blocking buffer consisting of PBS with Tween-20 (0.1%) and 1% nonfat dry milk. Membranes were then incubated with specific primary antibody (PKP2 monoclonal Fitzgerald, polyclonal Cx43 Millipore and phosphoCx43-S368 from Cell signaling) diluted in 1% nonfat dry milk overnight at 4°C followed by wash steps and secondary antibodies (Odyssey goat anti-mouse®680RD or anti-rabbit®800). Antigen complexes were visualized with the Odyssey Infrared Imaging System (LI-COR). The band intensity was quantified with ImageJ software.

To analyze expression levels of other proteins, LV and RV samples were homogenized as described in<sup>14</sup>. The homogenization buffer contained 0.9% NaCl, 10 mM Tris-HCl, 20 mM NaF, 2 µM leupeptin, 100 µM phenylmethylsulphonyl fluoride, 500 µM benzamidine and 100 nM aprotinin, pH 6.8. Following homogenization with a teflon pestle, samples were centrifuged at 1000 x g for 10 min at 4 °C. The supernatants were collected and stored at -80 °C until used. Protein concentrations were determined using the Bradford method (Bio-Rad). Fifty µg of protein from tissue homogenates were mixed with Laemlii buffer and separated by SDS-PAGE in 4-20% TGX gels (Bio-Rad). Proteins were transferred to PVDF membranes using the iblot2 system (Thermo

Fisher) or a conventional wet transfer. Membranes were probed using the ibind flex system (Thermo Fisher) with the following antibodies: anti-RyR2 (Thermo Fisher, MA3-925, 1:2000), SERCA2 (Thermo Fisher, MA3-919, 1:1000), PLB (Badrilla, A010-14, 1:5000), pT17-PLB (Badrilla, A010-13, 1:5000) and GAPDH (Millipore, MAB374, 1:10000). Secondary antibodies used were goat anti-mouse-HRP (Thermo Fisher, 31437, 1:1000) or goat-anti-rabbit-HRP (Thermo Fisher, 31463, 1:1000). Membranes were developed using SuperSignal ECL (Thermo Fisher) and imaged in a ChemiDoc MP Apparatus (Bio-Rad). Band intensity was calculated using ImageLab (Bio-Rad).

### **[<sup>3</sup>H]Ryanodine Binding Experiments**

[<sup>3</sup>H]Ryanodine binding experiments were performed as previously described<sup>2</sup>. Pools of three LV or RV samples were homogenized as described above for Western blot analysis. Binding mixtures contained 50 µg of protein from sample homogenates, 0.2 mM KCl, 20 mM Na-HEPES pH 7.4, 7 nM [<sup>3</sup>H]ryanodine (PerkinElmer), 1 mM EGTA and enough CaCl<sub>2</sub> to set free [Ca<sup>2+</sup>] between 10 nM and 10 µM. The Ca<sup>2+</sup>/EGTA ratio was determined with MaxChelator (WEBMAXCLITE v1.15, <http://maxchelator.stanford.edu>). Binding reactions were incubated for 2 h at 37 °C, then filtered through Whatman GF/B filters and washed with distilled water in a Brandel M24-R harvester. [<sup>3</sup>H]Ryanodine binding was determined by liquid scintillation in a TriCarb 4810 apparatus (PerkinElmer) using Bio-Safe II cocktail (RPI Corp). Corrections for non-specific binding were made in the presence of 20 µM unlabeled ryanodine (Enzo Life Sciences). Maximum binding and EC<sub>50</sub> were determined using Hill's sigmoidal fitting in Origin 2018b (Origin Lab).

### **Single molecule localization microscopy (SMLM) by stochastic optical reconstruction microscopy (STORM).**

Freshly isolated cardiomyocytes from control or PKP2cKO mice (14 days post-TAM) were plated on laminin-coated coverslips and left to adhere for at least 30 minutes before fixation (4% paraformaldehyde). Cells were then permeabilized with 0.1% Triton in PBS for 10 minutes. Blocking was done in PBS containing 2% Glycine, 2% BSA and 0.2% Gelatin, for 30 minutes. The primary Mouse monoclonal antibody against RyR (Thermo Fisher MA3-916), rabbit polyclonal against total Cx43 (EMD Millipore AB1728) or mouse N-cadherin (BD 610921) together with rabbit polyclonal against phosphoPKC-T638/641 were diluted 1:100 in blocking solution and incubated for 1 hour at room temperature. After three washes with PBS, the secondary antibody against Mouse conjugated with Alexa Fluor 647, Rabbit conjugated with Alexa Fluor 647 or a



combination of Mouse conjugated with Alexa Fluor 647 and Rabbit conjugated with Alexa Fluor 568 (1:10000, Invitrogen) were incubated for 1h at room temperature.

Samples were imaged using a custom-built platform based on an inverse microscopy setup (Leica DMI3000 as described before<sup>15</sup>. In brief, the 639 nm laser (UltraLaser, MRL-FN-639-800) was expanded (10×) and collimated into a 63× Objective (HCX PL APO, NA=1.47, Zeiss), and the illumination was configured to ~ 1.5 kW/cm<sup>2</sup> at a Highly Inclined illumination mode. The emitted fluorescence was collected by the same objective and further extended by 2 2× lens tubes (Diagnostic Instruments). The fluorescence was then filtered by a band-pass filter (FF01-676/37, Semrock) and recorded on a sCMOS camera (Prime 95B, Photometrics) at 33 Hz for 2000 frames. Imaging conditions were achieved by addition of 200 mmol/L mercaptoethylamine and an oxygen scavenging system (0.4 mg/ml glucose oxidase, 0.8 µg/mL catalase and 10% (wt/wt) glucose) to the fluorophore-containing sample.

Movies for each imaging were submitted to a home-built software in Matlab for precise single-molecule localization. In brief, each frame of the movie was convolved with a box function (box size = 4× FWHM of the 2D Gaussian PSF) and subtracted as background. The local maximums were then recognized and segmented into ~1.2×1.2 µm<sup>2</sup> squares. These squares were then submitted for 2D-Gaussian multi-PSF fitting (DAO-STORM)<sup>15</sup>. The fitting was performed using Nvidia GTX 1060 GPU via the Maximum Likelihood Estimation (MLE) algorithm. Note that the likelihood function was constructed by combining the Poisson shot-noise distribution and pre-calibrated pixel-specific Gaussian readout-noise distribution<sup>16</sup>. The localization accuracy of each fluorophore was then given as its Cramér-Rao Lower Bound (CRLB).

#### *Cluster analysis*

Reconstructed super-resolved images were processed with a smoothing filter (“Gaussian blur” function in ImageJ), adjusted for brightness and contrast and filtered to a threshold to obtain a binary image. For the experimental datasets, ROIs were manually drawn for each image and saved as an ImageJ ROI file. Cluster detection and parameters (size, circularity, etc) were obtained using the ImageJ function “Analyze particles”. The minimum size/area of contiguous pixels defined as a cluster was 4000 nm<sup>2</sup>. This represents an area of ten times our resolution and therefore was considered safely within the power of detection. Signal-positive areas of smaller dimensions were not included.

In order to standardize measurements and reduce the possibility of errors, an automated script was written to compute the distances between RyR clusters or from phosphoPK-T638/641 to the cell end. The images from the super-resolution fluorescence microscopy and their corresponding ROI files provided the input to the script. The script was written in Python and utilized the image processing packages scikit-image<sup>17</sup>, and “Mahotas,” an open source software for scriptable computer vision (<http://dx.doi.org/10.5334/jors.ac>). Two clusters were considered separate if one was at least 20 nm/1 pixel apart from another in any direction. The Origin program was used for data management.

#### *DBSCAN analysis (clustering algorithm)*

Analysis of the number of RyR units per cluster was achieved with the density-based clustering algorithm DBSCAN, which groups together points that are closely packed together (with many nearby neighbors), marking as outliers points that lie alone in low-density regions (nearest neighbors too far away). DBSCAN uses two input parameters—Eps and MinPts—and determines that a point is in a cluster if at least MinPts points are within a distance of Eps. We used an Eps value of 50 nm and a Minpts of 10 for DBSCAN analysis<sup>18</sup>. To calculate the cluster density, the number of fluorophores within each cluster was divided by the cluster area. The area of each cluster was approximated to an ellipse of which the longer and shorter arms were determined by Principle Component Analysis (PCA).

#### **Evaluation of membrane permeability in whole heart preparations**

Two fluorescent dyes, Lucifer Yellow (LY) and Rhodamine Dextran (RD), were used to quantify the entry of a small molecular weight dye into cells. Animal anesthesia and heart extraction was the same as described above for cell dissociation. Hearts were Langendorff-perfused at a constant flow rate of 2 mL/min with a low-calcium washing solution (WS) containing (in mM) 2 EGTA, 113 NaCl, 4.7 KCl, 1.2 MgSO<sub>4</sub>, 0.6 Na<sub>2</sub>HPO<sub>4</sub>, 0.6 KH<sub>2</sub>PO<sub>4</sub>, 12 NaHCO<sub>3</sub>, 10 KHCO<sub>3</sub>, 10 HEPES, 5.5 Glucose, 30 Taurine and enough CaCl<sub>2</sub> to adjust free [Ca<sup>2+</sup>] to 10 nM (MaxChelator), pH was adjusted to 7.40 with NaOH. The hearts were then perfused with a dye-added WS containing (in mg/mL): 1 LY (Sigma-Aldrich), 1 RD (Sigma-Aldrich), and 0.04 Wheat Germ Agglutinin Alexa Fluor 633 (WGA; Thermo Fisher) for 30 min at 37°C. Subsequently the dye in the extracellular space was washed by perfusion of the WS without EGTA and with 50 mL of 1.8 mM [Ca<sup>2+</sup>]; the exposure to low Ca<sup>2+</sup> was used to increase the probability of opening of Cx43 hemichannels<sup>19, 20</sup>, whereas the return to a Ca<sup>2+</sup>-containing solution intended to prevent the exit of the dye from the intracellular space before fixation<sup>20</sup>. Finally, the hearts were perfused with 10

mL of 4% paraformaldehyde (PFA) containing PBS and kept in the same solution (4% PFA) at 4°C for overnight. The PFA-fixed heart was placed in a petri dish filled with PBS, the epicardium was removed manually using forceps and the LV and RV free walls were separated and placed in contact with the glass bottom of the experimental chamber, epicardial-side down. LY (ex 405 nm; em 470-580 nm), RD (ex 543 nm; em 580-650 nm), and WGA (ex 633 nm; em 650-800 nm) fluorescence were observed in sequence with a Leica TCS SP5 confocal microscope (40× oil immersion lens). Imaging was performed at several randomly chosen sites in each tissue sample. We quantified LY fluorescence intensities in single cells separated by WGA signals, from all cells in the images, by using LAS X software. In some experiments, the hearts were perfused with dye-containing solution (w/ 1.8 mM Ca<sup>2+</sup>) for 5 min and then immediately imaged to confirm that the LY and RD molecules reached the extracellular space of the tissue.

### **Cx43 hemichannel block with TAT-Gap 19**

Cx43 hemichannels were blocked by incubation with TAT-Gap 19 (GAP19) for 1 hour at a concentration of 20 μM. This molecule was used as one of the methods to document the role of Cx43 hemichannels on the changes in Ca<sup>2+</sup> homeostasis in PKP2cKO-RV myocytes, as specified in the text.

### **Electrophysiological measurements**

#### *Cell capacitance*

To measure the cell membrane capacitance  $C_m$ , the current transient was recorded in response to 10 msec voltage step to -90 mV from holding potential -80 mV after establishing whole-cell configuration. The recording pipette solution contained (in mmol/l): KCl 135, MgCl<sub>2</sub> 1, EGTA 10, HEPES 10, and glucose 5, pH 7.2 with KOH. The bath solution contained (in mmol/l): NaCl 136, KCl 4, CaCl<sub>2</sub> 1, MgCl<sub>2</sub> 2, CdCl<sub>2</sub> 0.2, HEPES 10, and glucose 10, pH 7.4 with NaOH. The  $C_m$  was determined by the equation:  $C_m = Q/\Delta E$ , where the charge  $Q$  can be obtained by integrating the area under the current transient and  $\Delta E$  was 10 mV.

#### *Whole-cell NCX current recording*

NCX current was measured using an external solution containing (in mmol/l): 140 NaCl, 1.0 CaCl<sub>2</sub>, 1 MgCl<sub>2</sub>, 10 HEPES, 10 Glucose, 5 CsCl, 0.01 Nifedipine, 0.05 Oubain, 1 BaCl<sub>2</sub>, pH 7.4 (NaOH). The recording pipettes were filled with a solution containing (in mmol/l): 20 NaCl, 65 CsCl, 20 TEA-Cl, 6 CaCl<sub>2</sub>, 10 EGTA, 5 MgATP and 10 HEPES, pH 7.25 with CsOH. The peak NCX current

density was measured at the 2000 ms test pulse to +60 mV from -30 mV holding potential and five sweeps before and after NiCl<sub>2</sub> (5 mM) application were averaged and subtracted<sup>21</sup>.

## **Electron Microscopy**

### *Sample Preparation*

Mice were anesthetized with sodium pentobarbital, perfused with 4% paraformaldehyde in PBS and then euthanized by excision of the heart. The perfused heart was cut into 1mm<sup>3</sup> and placed in a fixative solution containing 2% paraformaldehyde and 2.5% glutaraldehyde in phosphate buffer (PB, pH7.2). Fixed mouse heart was continue processed with modified OTTO<sup>22</sup>, and embedded in Durcupan. In brief, the heart tissue was washed with 0.1M PB, post fixed in 2% OsO<sub>4</sub>/ 1.5% potassium ferrocyanide for 1.5 h at room temperature, then stained with freshly made 1% tannic acid (EMS) in PB for two consecutive steps with 2 hours each step at 4°C to allow for additional staining. The tissue was then washed in ddH<sub>2</sub>O, placed in 2% aqueous OsO<sub>4</sub> for 40 min at room temperature, and *en bloc* stained in 1% aqueous uranyl acetate at 4°C overnight. The tissues were then washed with ddH<sub>2</sub>O, dehydrated in a series of ethanol solutions (30, 50, 70, 85, 95, 100, 100%; 10 min each, on ice) and replaced with ice-cold dry acetone for 10 min, followed by 10 min in acetone at room temperature. The sample was gradually equilibrated with Durcupan ACM Araldite embedding resin (Electron Microscopy Sciences, EMS, PA) and embedded in fresh made 100% Durcupan.

### *Serial Block-Face Scanning Electron Microscopy (SBF-SEM)*

The sample block was trimmed and thin sections were cut on slot grids to identify the area of interest. The sample block was then mounted on an aluminum specimen pin (Gatan, Pleasanton, CA) using silver conductive epoxy (Ted Pella Inc.) to electrically ground tissue block. The specimen was trimmed again with pyramid shape and coated with a thin layer of gold/palladium (Denton Vacuum DESK V sputter coater, Denton Vacuum, LLC., NJ, USA). Serial block face imaging was performed using Gatan OnPoint BSE detector in a Zeiss GEMINI 300 VP FESEM equipped with a Gatan 3View automatic microtome unit. The system was set to cut sections with 100nm thickness, imaged with gas injection setting at 65% (3.9E-03mBar) with Focus Charge Compensation to reduce the charge, and images were recorded after each round of section from the block face using the SEM beam at 1.2 keV with a dwell time of 1.0 μs/pixel. Each frame is 20 x25 μm with pixel size of 2nm. Data acquisition occurred in an automated way using the Auto Slice and View G3 software. A stack of 150 slices was aligned, assembled using ImageJ, with a volume of roughly 20x25x15μm<sup>3</sup> dimensions was obtained from the tissue block.

## **Optical mapping of epicardial activity in Langendorff-perfused heart preparations using voltage sensitive dyes**

Mice were heparinized (heparin sodium, 0.5 U/g IP) and euthanized by CO<sub>2</sub> inhalation followed by cervical dislocation. Hearts were isolated and Langendorff perfused with modified Tyrode's solution as previously described [1,2]. The excitation-contraction uncoupler Blebbistatin (Enzo Life Sciences, 4 mg/L) was added to the perfusate to limit motion artifacts during optical recordings. Volume conducted ECGs were continuously recorded. Fluorescent signals were recorded using a modified microscope (MVX10 Olympus) equipped for epifluorescent illumination. Images were acquired with a CMOS camera (SciMedia MiCAM ULTIMA) at 1,000 frames/s with 14-bit resolution from a 100 × 100-pixel array. Dyes were excited with a 530 nm mounted LED (ThorLabs). The emission filters used for voltage and calcium mapping were 610 nm long pass and 593±20 nm band pass, respectively. Hearts were stained with the voltage sensitive dye di-4-ANEPPS and perfused with isoproterenol (100nM) in modified Tyrode's solution. A programmed arrhythmia stimulation protocol consisting of 10 second long burst stimulation followed by a 30 second wait period was applied to the right ventricular free wall. Burst stimulation basic cycle lengths ranged from 60 to 20 ms in 5 ms decrements. Images were acquired from the right ventricular free wall and analyzed using custom software as previously described<sup>23-26</sup>.

## **Echocardiographic analysis**

Transthoracic echocardiography was performed using a Vevo2100 Imaging System (VisualSonics Inc., Toronto, Canada) with a 30 MHz probe, as described in<sup>2</sup>. Briefly, after induction of anesthesia in a chamber containing isoflurane 4-5% in oxygen, the mouse was positioned supine on a heat pad in order to maintain body temperature at 37-38 °C and anesthesia was maintained with 1.5% isoflurane in 700 ml O<sub>2</sub>/minute via a nose-cone. For right ventricle area measurements, images were acquired in a modified parasternal long-axis view (B-mode): during diastole, the diameter was measured half-way between the pulmonary and tricuspid valves from the free wall to the interventricular septum and the area subsequently calculated.

## **Statistical analysis**

Numerical results are given as means ± standard error of the mean (S.E.M.). Two-way repeated measures ANOVA followed by Bonferroni post-test was used for most data sets. In specific cases (noted in the respective figure legends), paired or unpaired Student's *t*-test, one-way repeated

measures ANOVA-Bonferroni or Chi-square test was used. Analysis was done using OriginPro 8, Origin 2018b, SPSS 25 and SigmaPlot 13 packages. Differences were considered to be significant at  $p < 0.05$ . Hierarchical analysis was carried out as indicated in Figure legends, based on the work of Sikkel et al<sup>27</sup>, utilizing the open source package thereby provided. Of note, this resource first detects adequacy of hierarchical analysis vis a vis other methods; analysis was carried out accordingly for each data set.

## FIGURE LEGENDS FOR ONLINE- ONLY DATA SUPPLEMENT

### ONLINE-ONLY DATA SUPPLEMENT

**Figure I. Left ventricular ejection fraction (LVEF) in heterozygous PKP2-deficient mice.** A total of 6 Cre-positive, PKP2<sup>fl/wt</sup> mice were injected with tamoxifen (TAM) using the protocol described in “Methods”. These animals, heterozygous-deficient for PKP2, were followed for a total of 84 days post-TAM injection (DPI; abscissae) to examine whether TAM-induced Cre-expression had in itself a deleterious effect on life expectancy or heart function. As opposed to plakophilin-2 conditional knockout (PKP2cKO) mice, this group showed 100% survival and no apparent differences in left ventricular function (as a reference, PKP2cKO animals show a significant drop in LVEF by day 28, and none of the injected animals have survived past day 50, as previously reported<sup>2</sup>).

**Figure II. Early and delayed after-transients in plakophilin-2 conditional knockout (PKP2cKO) myocytes.** Left panels: Time space plots and time course of Ca<sup>2+</sup> transients recorded from PKP2cKO-right ventricular (RV) myocytes showing early after transients (EATs; **A**), delayed after transients (DATs; **C**) and spontaneous Ca<sup>2+</sup> waves (**E**). Right panels: Bar graphs; quantification of EATs (**B**), DATs (**D**) and spontaneous Ca<sup>2+</sup> waves (**F**), presented as percent of cells where the transient was recorded. Total number of cells studied for each group: *n*=49 left ventricular (LV) cells, 51 RV cells from 9 control mice, and *n*=55 LV cells, 55 RV cells from 11 PKP2cKO mice. \*\**p*<0.01 vs. control; †*p*<0.05 vs. LV. Chi-squared test was used to examine the relationship between categorical variables.

**Figure III. Western blot analysis.** **A:** plakophilin-2 (PKP2) immunodetection in plakophilin-2 conditional knockout (PKP2cKO) and control (Ctrl) mice 14 days post- tamoxifen (TAM). Western blot shows similar abundance of PKP2 in left ventricle (LV) and right ventricle (RV) of Ctrl mice and an equal and drastic reduction in PKP2cKO. A remnant PKP2 is detected in the PKP2cKO samples, likely originating from non-myocyte cells in the heart lysate. Average normalized band intensities shown in **B** (Mean±standard error of the mean; SEM; *n*=3). **C:** ryanodine receptor 2 (RyR2), sarco/endoplasmic reticulum Ca<sup>2+</sup>-ATPase 2 (SERCA2), phospholamban (PLB) and T17-PLB immunodetection in PKP2cKO and control (Ctrl) mice 14 days post-TAM. Average normalized band intensities shown in **D-G**. (Mean±SEM). Black bars correspond to Ctrl hearts. Data from PKP2cKO hearts is depicted in red. Band densities were normalized to glyceraldehyde 3-phosphate dehydrogenase (GAPDH) in each lane. Small numbers in the bars indicate *n* values

(separate lanes). For RyR2: Ctrl-LV vs Ctrl-RV and PKP2cKO-RV vs PKP2cKO-LV:  $^{**}p < 0.01$ . For SERCA2a: PKP2cKO-LV vs PKP2cKO-RV  $^{\dagger}p < 0.05$ . Two-way repeated measures analysis of variance (ANOVA)-Bonferroni test.

**Figure IV. Peak NCX current density.** Peak  $\text{Na}^+$ - $\text{Ca}^{2+}$  exchange (NCX) current density at fixed  $\text{Ca}^{2+}$  and  $\text{Na}^+$  concentrations was unchanged in left ventricle (LV) and right ventricle (RV) of control (Ctrl) and plakophilin-2 conditional knockout (PKP2cKO) samples. Voltage clamp protocol in the detailed Methods section. Black bars correspond to Ctrl hearts and red bars correspond to PKP2cKO (Mean  $\pm$  standard error of the mean; SEM). Number of recorded cells indicated within each bar. Cells obtained from 3 control and 4 PKP2cKO animals.

**Figure V. Right versus left transcriptomic analysis in control and PKP2cKO mice. A:** Top: Volcano plot of upregulated or down-regulated transcripts in the right ventricle (RV) (relative to left ventricle; LV) of control hearts. Red dots correspond to transcripts with  $\text{Log}_2\text{FC} > \pm 1.0$  and  $-\log_{10}(\text{FDR}) > 2$  ( $\text{padj} < 0.01$ ); Blue dots:  $\text{Log}_2\text{FC}$  between 0 and  $\pm 1.0$  and  $-\log_{10}(\text{FDR}) > 2$ ; Grey dots: transcripts with  $\log_{10}(\text{FDR}) < 2$ . Transcripts corresponding to the red dots are listed in the bottom panel.  $n = 5$  mice. FDR: false discovery rate. **B:** Same as **A** but in this case, samples were obtained from 5 plakophilin-2 conditional knockout (PKP2cKO) mice 14 days post-tamoxifen (TAM). Only nine transcripts in the PKP2cKO group met criteria for significance and magnitude of differential, and four of them were also differentially expressed in the control (Ctrl), as examined by paired comparisons, analyzed by paired  $t$ -tests corrected by the Benjamini and Hochberg method. Consistent with the fact that no major differences in transcript abundance were detected between groups, a principal component analysis (PCA) did not produce a defined segregation of experimental sets into separate clusters. In other words, the PCA predicted that there was insufficient variability between samples to discriminate them statistically, in agreement with the results obtained through the paired  $t$ -test comparisons. Complete datasets can be found in the accompanying Table I and Table II in the online-only supplemental data section. ribonucleic acid sequencing (RNAseq) data analysis carried out using the DESeq2 package (<https://bioconductor.org/packages/release/bioc/html/DESeq2.html>).

**Figure VI. Distribution histogram of fraction of the total number of RyRs (Frequency %) as a function of the number (No.) of ryanodine receptor 2 (RyR2) per cluster in control (Ctrl; black) and plakophilin-2 conditional knockout (PKP2cKO) left and right ventricles (red).**



The Ctrl group shows a larger peak in the 10-25 range, while the PKP2cKO group shows a broader distribution. Values specified in Supplemental Figure VII.

**Figure VII. Median and mean number of ryanodine receptor 2 (RyR2) molecules per cluster, and average cluster size  $\pm$  standard error of the mean (in nm<sup>2</sup>) in each condition.** Parameters were calculated using Density-Based Spatial Clustering of Applications with Noise (DBSCAN) analysis. Total number of clusters analyzed (clusters that have at least 10 RyRs):  $n=32738$  RyR2 clusters from left ventricular (LV) myocytes and 16595 clusters from right ventricular (RV) myocytes from control; 1666 LV and 4396 RV clusters from PKP2cKO mice. Two-way repeated measures analysis of variance (ANOVA)-Bonferroni, \*\*\* $p<0.001$  vs. control, ††† $p<0.001$  vs. LV.

**Figure VIII. Ryanodine receptor 2 (RyR2) abundance in samples used to calculate [<sup>3</sup>H]Ryanodine binding. A:** The term “Ctrl” refers to samples from control animals. “cKO” refers to samples obtained from plakophilin-2 conditional knockout (PKP2cKO) animals, 14 days post-tamoxifen (TAM). R: right ventricle, L: left ventricle. **B:** Average normalized expression.  $n=4$  for each group. Each “n” is a pool of samples obtained from 3 hearts. LV: left ventricle. RV: right ventricle. \* $p<0.05$  vs. control. Two-way repeated measures analysis of variance (ANOVA)-Bonferroni test.

**Figure IX. Alignment of the phosphorylation hotspot of RyR2 and the potential protein kinase C (PKC) target at Thr2809. A:** Alignment of the “phosphorylation hotspot” of ryanodine receptor 2 (RyR2) for the species noted in the left. Accession numbers from Uniprot ([www.uniprot.org](http://www.uniprot.org)). The pig sequence was reconstructed from previous publications<sup>28</sup>. Flanking numbers correspond to the RyR2 sequence number for each species. The red “T” marks the preservation of the threonine residue. Serines 2807 and 2813, known as kinase substrates, are noted in green. **B:** RyR2 sequence as a potential substrate for PKC phosphorylation, based on the consensus motifs of the various PKC isoforms.

**Figure X. Ca<sup>2+</sup> content in the intracellular compartments. A:** Confocal line-scan images (1.43 ms/line) recorded from permeabilized myocytes isolated from the left ventricle (LV) or the right ventricle (RV) free wall of either control (Ctrl) or plakophilin-2 conditional knockout (PKP2cKO) mice 14 days post- tamoxifen (TAM). In this and other panels, the pulse of caffeine (10 mM) is indicated by the orange bar at the bottom of the image. **B:** Time course and amplitude of the change in fluorescence during and immediately following the caffeine pulse. Notice the larger

amplitude of the transient recorded from PKP2cKO RV myocytes. Cumulative data are shown in **C**. Number of experiments noted in the bar graphs. Cells originated from three different mice in each group (Ctrl or PKP2cKO). \*\*\* $p < 0.001$  vs. control, † $p < 0.05$  vs. LV. Two-way repeated measures analysis of variance (ANOVA)-Bonferroni test.

**Figure XI. Temperature-dependent loading of Rhod-2 into mitochondria of isolated adult cardiomyocytes.** **A:** Ventricular myocytes were loaded with 2  $\mu\text{M}$  Rhod-2 AM in 37°C for 5 h and then labeled with 200 nM MitoTracker Deep Red FM (fluorescent molecules) for additional 10 min (37°C). Rhod-2 (**Aa**) and MitoTracker (**Ab**) fluorescence signals visualized with confocal fluorescence imaging. Merged image (**Ac**) of the Rhod-2 and MitoTracker signals showed that, when loading at warm temperatures, Rhod-2 was predominantly localized to the cytoplasm rather than in the mitochondria. **B:** Ventricular myocytes were loaded with 2  $\mu\text{M}$  Rhod-2 AM in 4°C for 1 h and followed by 37°C for 4 h and then labeled with 200 nM MitoTracker Deep Red FM for additional 10 min (37°C). Rhod-2 (**Ba**) and MitoTracker (**Bb**) fluorescence signals visualized with confocal fluorescence imaging. Merged image (**Bc**) of the Rhod-2 and MitoTracker signals showed that Rhod-2 was selectively loaded to the mitochondria. This latter protocol was used for the experiments reported in Figure 5 of the manuscript.

**Figure XII. SR load as a function of extracellular  $\text{Ca}^{2+}$  in PKP2cKO-RV myocytes.** Panel **A:** time-space plots showing  $\text{Ca}^{2+}$  transients elicited by a pulse of caffeine (same protocol as in Figure 5A of the main manuscript). Time course in Panel **B**. Data obtained from a plakophilin-2 conditional knockout (PKP2cKO)-right ventricular (RV) cell recorded at 1.8 mM  $[\text{Ca}^{2+}]_o$  (left) and from a separate PKP2cKO-RV cell recorded at 0.6 mM  $[\text{Ca}^{2+}]_o$ . As shown by the cumulative data in panel **C**, decreasing  $[\text{Ca}^{2+}]_o$  to 0.6 mM equalized the amplitude of the caffeine-induced transient to a level comparable to that observed in control or in PKP2cKO-left ventricle (LV) at  $[\text{Ca}^{2+}]_o$  1.8 mM. Data for RV and LV controls and PKP2cKO are reproduced from Figure 5A for comparison. For the PKP2cKO-RV at 0.6 mM  $[\text{Ca}^{2+}]_o$ ,  $n=15$  from 3 mice. # $p < 0.05$  vs. PKP2cKO RV in 1.8  $[\text{Ca}^{2+}]_o$ . Two-way repeated measures analysis of variance (ANOVA)-Bonferroni test.

**Figure XIII. Dye uptake assay in intact heart.** **A:** A murine adult heart was Langendorff-perfused with a solution containing Lucifer Yellow (LY) and Rhodamine Dextran (RD) and then immediately imaged by confocal microscopy. Notice that both dyes are abundantly localized to the interstitial/capillary space. In contrast, **B** shows a confocal image of a heart loaded with LY, RD and Wheat Germ Agglutinin (WGA), subsequently washed with dye-free solution and then fixed

in paraformaldehyde (PFA) overnight. Note that Rhodamine Dextran (average molecular weight ~10,000) was not loaded in the cells and was removed by the wash, indicating that Lucifer Yellow did not enter the cells through the damaged sarcolemma.

**Figure XIV. Abundance and localization of Cx43 is unaltered in PKP2cKO mice at 14 days post-tamoxifen (TAM).** Western blot examples are shown in the upper left panel (**A**), and the results of densitometry analysis are shown in the bar graphs (**B**). Methods in the “Detailed Methods” section. Number of hearts: 9 and 8 for control (Ctrl) and plakophilin-2 conditional knockout (PKP2cKO), respectively. GAPDH: glyceraldehyde 3-phosphate dehydrogenase. **C**: Stochastic optical reconstruction microscopy (STORM)-acquired images of Cx43 in single myocytes dissociated from left ventricle (LV) or right ventricle (RV) of Ctrl or PKP2cKO mice 14 days post-TAM (scale bar 5  $\mu$ m). **D**: Enlargement of the yellow-boxed areas in **C** showing part of the cell ends (scale bar in insets, 2  $\mu$ m). **E**, **F** and **G**: Average size, cluster density and cluster circularity (1.0 indicates perfect circle) of Cx43 clusters in control and PKP2cKO myocytes measured at the cell end. Control:  $n=15$  LV cells; and 14 RV cells from 2 mice. PKP2cKO:  $n=14$  LV cells; and 17 RV cells from 2 mice. The results show no differences between the groups when examined by two-way repeated measures analysis of variance (ANOVA)-Bonferroni.

**Figure XV. Membrane permeability to Lucifer Yellow and effect of Cx43 expression in plakophilin-2 conditional knockout (PKP2cKO) hearts 21 days post-tamoxifen (TAM).** **A**: Confocal images collected from the epicardial phase of either the left ventricular (LV) or the right ventricular (RV) free wall of hearts harvested from control (Ctrl), PKP2cKO mice 21 days post-TAM (PKP2cKO) or a conditional knockout of PKP2 also heterozygous conditional for Cx43 (i.e., PKP2cKO/Cx43+/-), also at 21 days post-TAM. Images were obtained after a 30-min perfusion with 1 mg/mL Lucifer Yellow (LY; MW 457; green), 1 mg/mL Rhodamine Dextran (RD; MW ~10,000) and 0.04 mg/mL Wheat Germ Agglutinin (WGA; red) in 10 nM free  $[Ca^{2+}]$  solution (see “Methods” for further details). Image fields were chosen at random and the intensity of the LY fluorescence (in a scale 0-225) was measured within regions of interest (ROIs) that excluded areas voided of cells. MW: molecular weight. **B**: Average LY intensity measured from cells in the following groups: Control (Ctrl; black bars;  $n=327$  LV cells, 395 RV cells from 2 mice), PKP2cKO (red bars;  $n=348$  LV cells, 415 RV cells from 2 mice) and PKP2cKO/Cx43+/- (green bars;  $n=690$  LV cells, 291 RV cells from 2 mice). \*\*\* $p<0.001$  vs. control; ### $p<0.001$  vs. PKP2cKO. Two way repeated measures analysis of variance (ANOVA)-Bonferroni.

**Figure XVI. Effect of TAT-Gap19 on cell permeability to Lucifer Yellow (LY).** Left: single myocyte maintained in  $\text{Ca}^{2+}$ -free solution and exposed to LY. Notice fluorescence emitted from the intracellular space. Right: Same experiment but in the presence of transactivator of transcription (TAT)-Gap19. Notice the absence of fluorescence emission, likely consequent to inhibition of Cx43 hemichannel activity.

**Figure XVII. Echocardiographic measurements.** Echocardiographic measurements of right ventricular area of PKP2cKO/Cx43 $\pm$  mice, compared to plakophilin-2 conditional knockout (PKP2cKO) (the latter dataset also reported in<sup>2</sup> numbers in the bars indicate number of animals tested). RV: right ventricle; TAM: tamoxifen.  $^{##}p < 0.01$  by unpaired *t*-test. Only one comparison between two variables (RV Area PKP2cKO vs. PKP2cKO/Cx43 $\pm$  at 14 days post-TAM).

**Figure XVIII. Analysis of cell morphology.** In all panels, black and red bars correspond to data from control and plakophilin-2 conditional knockout (PKP2cKO) myocytes, respectively. **A:** Isolated cells were recorded to measure cell capacitance by the procedure detailed in Methods. Separately, cell morphology was determined by light microscopy to measure surface area (**B**), cell length and width (**C**, **D**) and sarcomere length (**E**). The results show no differences between the groups. Numbers in the bars indicate *n* values of cells tested. 4 mice were used for each group.

**Figure XIX. Analysis of phosphoPKC-T638/641 clustering using single molecule-localization microscopy single molecule localization microscopy (SMLM) by stochastic optical reconstruction microscopy (STORM)** **A:** STORM-acquired images of phosphoPKC-T638/641 (in green; pPKC) and N-cadherin (in red; Ncadh) in single myocytes dissociated from left ventricle (LV) or right ventricle (RV) of control (Ctrl) or plakophilin-2 conditional knockout (PKP2cKO) mice 14 days post-TAM (scale bar 5  $\mu\text{m}$ ). TAM: tamoxifen. **B:** Enlargement of the yellow-boxed areas in A showing the cell ends (scale bar in insets, 2  $\mu\text{m}$ ). **C** and **D:** Average cluster size and cluster density of phosphoPKC clusters in control and PKP2cKO myocytes measured at the cell ends. **E:** Distances from phosphoPKC clusters to the cell end marked as N-cadherin (measured in nm). *n*=692 clusters from 27 LV cells; 815 clusters from 28 RV cells, from 3 mice. PKP2cKO: *n*=596 clusters from 33 LV cells; 524 clusters from 31 RV cells, from 3 mice. Statistical significance by two-way repeated measures analysis of variance (ANOVA)-Bonferroni, \**p*<0.05 vs. control,  $^{\dagger}p < 0.05$  vs. LV,  $^{***}p < 0.001$  vs. control, and  $^{\dagger\dagger\dagger}p < 0.001$  vs. LV.

**Figure XX. Intercalated disc ultrastructure.** **A:** Single frame of a complete focused ion beam-scanning electron microscopy (FIB-SEM)-acquired set showing the ultrastructure of the intercalated disc from a control (Ctrl; left panel) and a plakophilin-2 conditional knockout (PKP2cKO; right panel) right ventricle (RV) tissue, 14 days post-tamoxifen (TAM). Scale bar: 2  $\mu\text{m}$ . Enlarged images (yellow-boxed areas) are shown in **B** (Scale bar: 0.5  $\mu\text{m}$ ). Notice increased intercellular distance in the sample from PKP2cKO-RV. A complete 3D volume is presented in supplemental videos 1 and 2.

**Figure XXI. High-resolution optical mapping of electrical activation in Langendorff-perfused hearts.** **A:** Volume-conducted electrocardiogram (ECG) showing sinus rhythm. **B:** Volume-conducted ECG obtained after burst stimulation of the right ventricle (RV) free wall. Notice run of ventricular tachycardia after burst, and spontaneous self-termination. **C-top:** Optical pseudo-ECG obtained from the RV free wall during a triggered polymorphic ventricular tachycardia. **C-Bottom:**  $dF/dt$  maps showing propagation of the electrical wavefront at two time windows (1 and 2 as marked in C-top). Data were acquired after 1 minute of perfusion with a solution containing 100 nM Isoproterenol. A total of 4 hearts were tested for each group. Ventricular arrhythmias were recorded in all 4 plakophilin-2 conditional knockout (PKP2cKO) hearts and in none of the controls. Scale bar: 1 mm. Experimental protocol detailed in the “Methods” section.

**Supplemental video 1 and 2:** Focused ion beam-scanning electron microscopy (FIB-SEM)-resolved three-dimensional ultrastructure from Control and plakophilin-2 conditional knockout (PKP2cKO) right ventricle respectively.

**Supplemental table 1:** Ribonucleic acid sequencing (RNAseq) dataset for right and left ventricles of control mouse hearts at 14 days post-injection. Padj: p adjusted value for false discovery rate.

**Supplemental table 2:** Ribonucleic acid sequencing (RNAseq) dataset for right and left ventricles of plakophilin-2 conditional knockout (PKP2cKO) mouse hearts at 14 days post-injection. Padj: p adjusted value for false discovery rate.

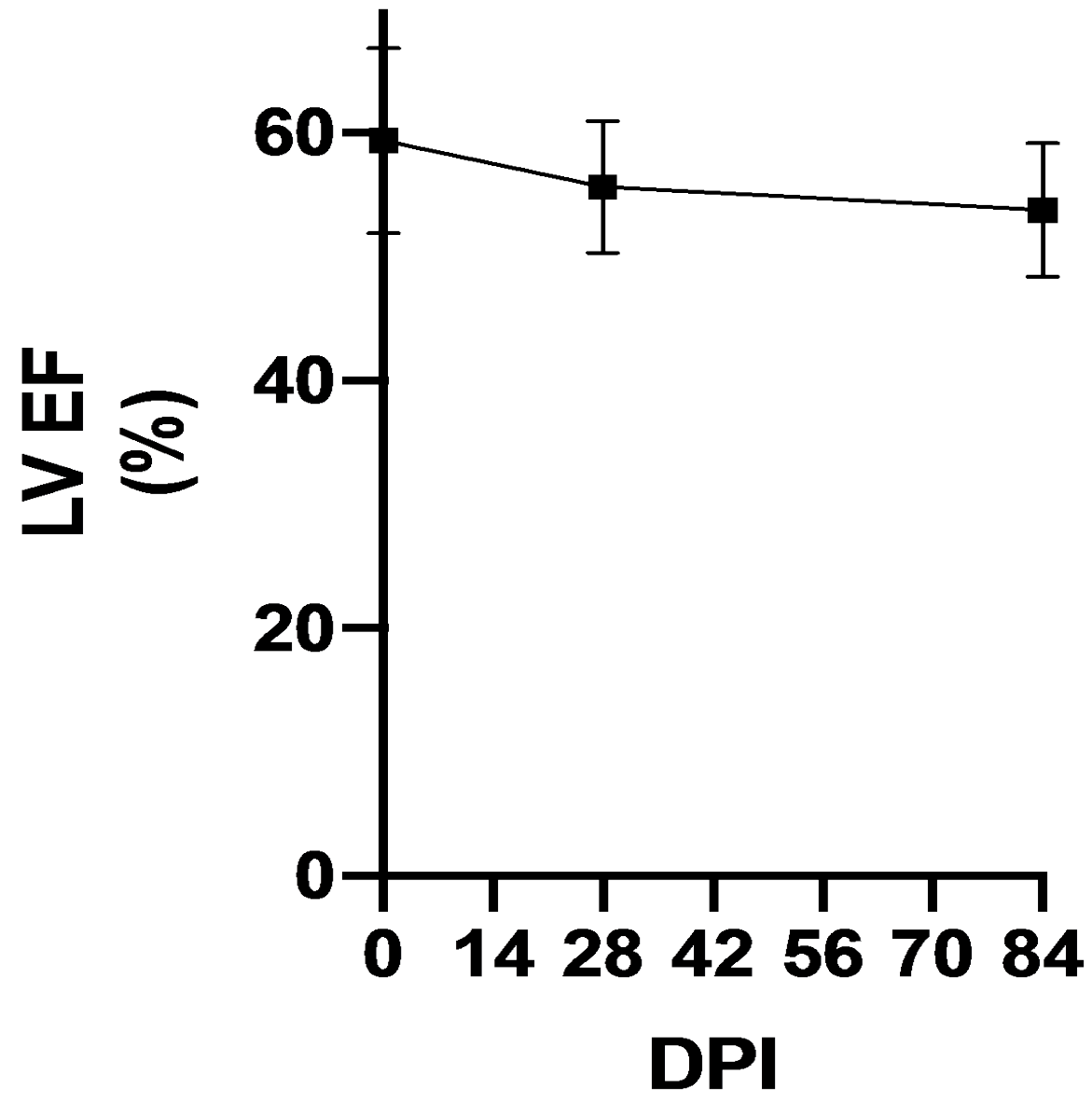
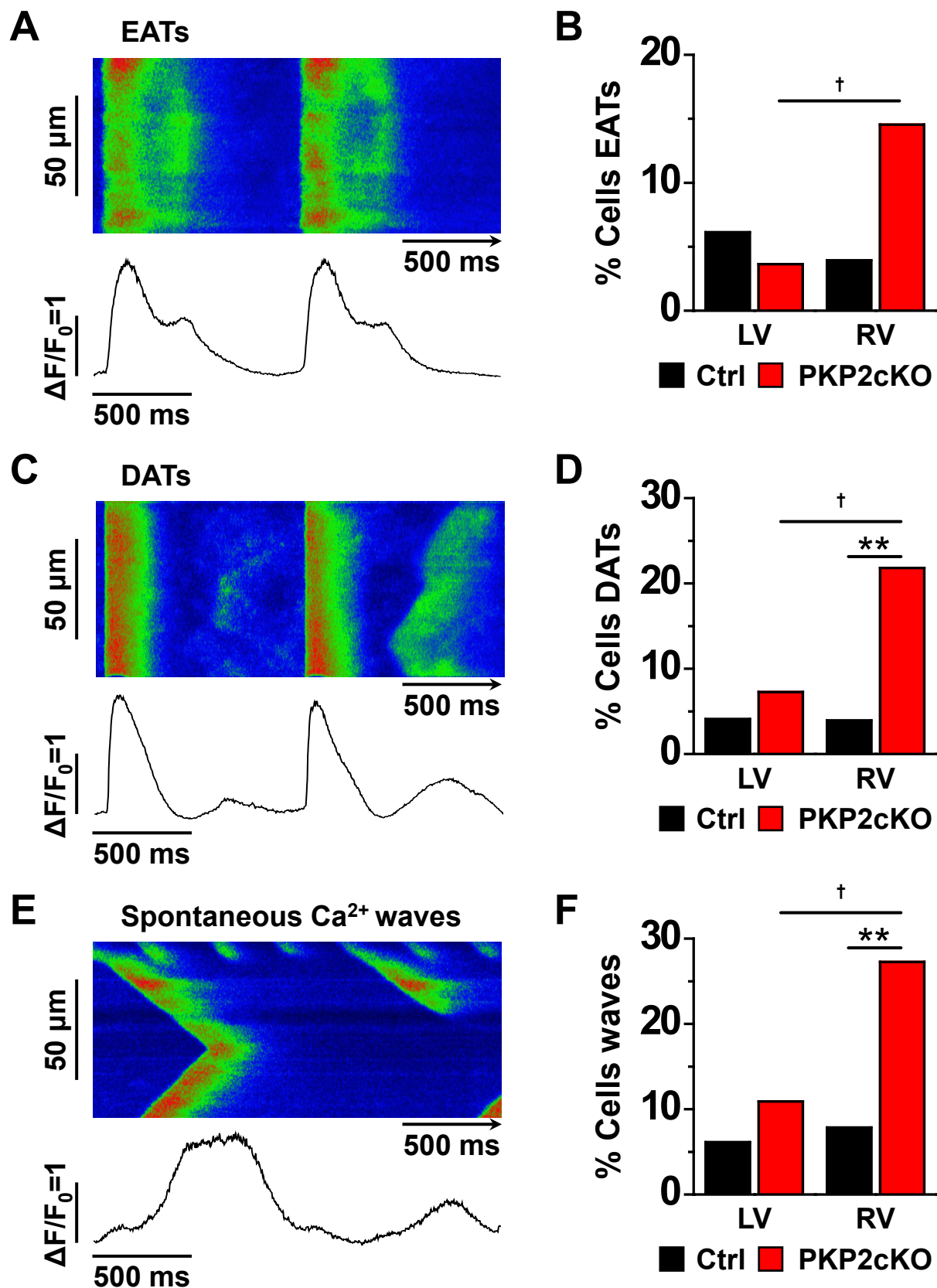


**Figure I. Left ventricular ejection fraction (LVEF) in heterozygous PKP2-deficient mice.** A total of 6 Cre-positive, PKP2<sup>fl/wt</sup> mice were injected with tamoxifen (TAM) using the protocol described in “Methods”. These animals, heterozygous-deficient for PKP2, were followed for a total of 84 days post-TAM injection (DPI; abscissae) to examine whether TAM-induced Cre-expression had in itself a deleterious effect on life expectancy or heart function. As opposed to plakophilin-2 conditional knockout (PKP2cKO) mice, this group showed 100% survival and no apparent differences in left ventricular function (as a reference, PKP2cKO animals show a significant drop in LVEF by day 28, and none of the injected animals have survived past day 50, as previously reported<sup>2</sup>).



Supplemental figure II



**Figure II. Early and delayed after-transients in plakophilin-2 conditional knockout (PKP2cKO) myocytes.** Left panels: Time space plots and time course of Ca<sup>2+</sup> transients recorded from PKP2cKO-right ventricular (RV) myocytes showing early after transients (EATs; **A**), delayed after transients (DATs; **C**) and spontaneous Ca<sup>2+</sup> waves (**E**). Right panels: Bar graphs; quantification of EATs (**B**), DATs (**D**) and spontaneous Ca<sup>2+</sup> waves (**F**), presented as percent of cells where the transient was recorded. Total number of cells studied for each group: *n*=49 left ventricular (LV) cells, 51 RV cells from 9 control mice, and *n*=55 LV cells, 55 RV cells from 11 PKP2cKO mice. \*\**p*<0.01 vs. control; †*p*<0.05 vs. LV. Chi-squared test was used to examine the relationship between categorical variables.

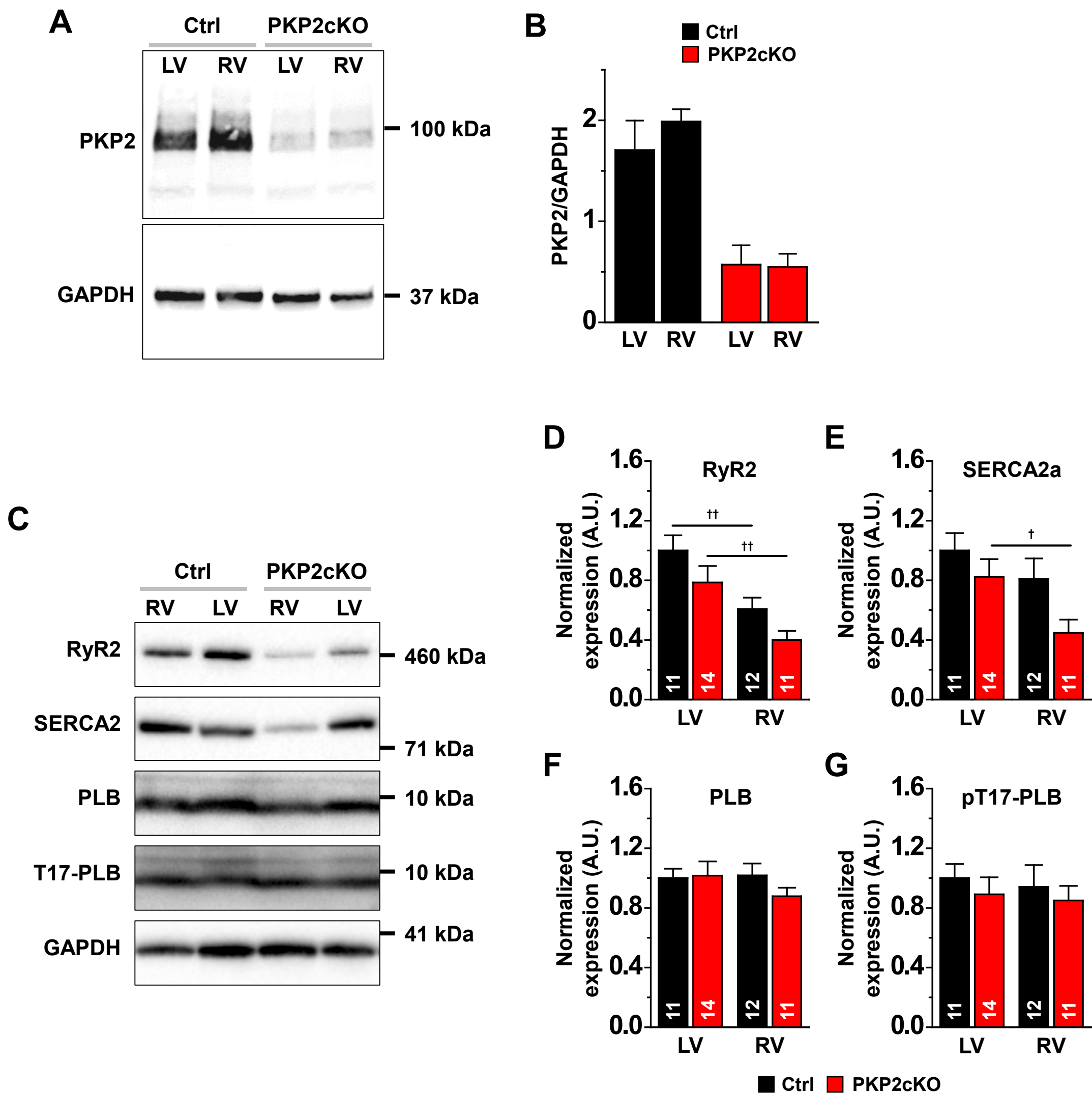
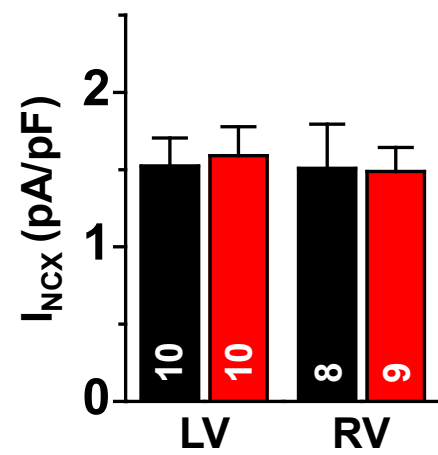
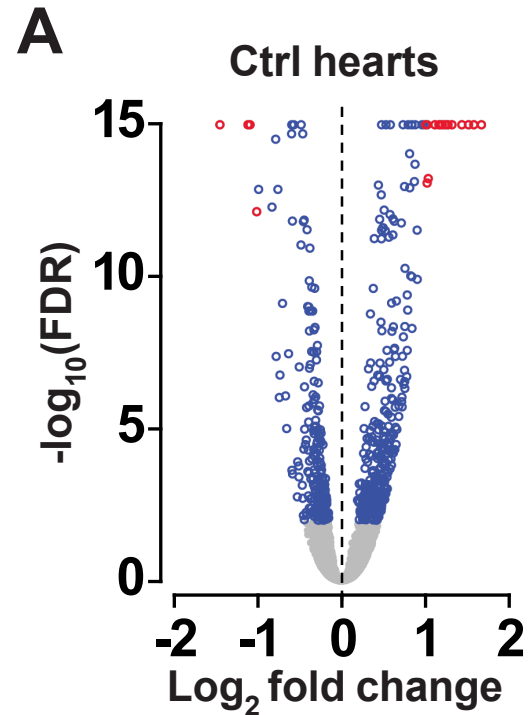


**Figure III. Western blot analysis.** **A:** plakophilin-2 (PKP2) immunodetection in plakophilin-2 conditional knockout (PKP2cKO) and control (Ctrl) mice 14 days post- tamoxifen (TAM). Western blot shows similar abundance of PKP2 in left ventricle (LV) and right ventricle (RV) of Ctrl mice and an equal and drastic reduction in PKP2cKO. A remnant PKP2 is detected in the PKP2cKO samples, likely originating from non-myocyte cells in the heart lysate. Average normalized band intensities shown in **B** (Mean±standard error of the mean; SEM;  $n=3$ ). **C:** ryanodine receptor 2 (RyR2), sarco/endoplasmic reticulum  $\text{Ca}^{2+}$ -ATPase 2 (SERCA2), phospholamban (PLB) and T17-PLB immunodetection in PKP2cKO and control (Ctrl) mice 14 days post-TAM. Average normalized band intensities shown in **D-G**. (Mean±SEM). Black bars correspond to Ctrl hearts. Data from PKP2cKO hearts is depicted in red. Band densities were normalized to glyceraldehyde 3-phosphate dehydrogenase (GAPDH) in each lane. Small numbers in the bars indicate  $n$  values (separate lanes). For RyR2: Ctrl-LV vs Ctrl-RV and PKP2cKO-RV vs PKP2cKO-LV:  $^{\dagger}p<0.01$ . For SERCA2a: PKP2cKO-LV vs PKP2cKO-RV  $^{\dagger}p<0.05$ . Two-way repeated measures analysis of variance (ANOVA)-Bonferroni test.

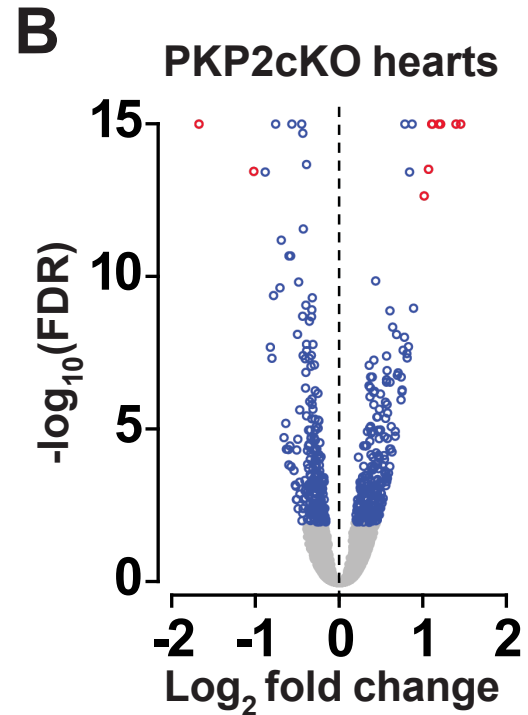


Supplemental figure IV

**Figure IV. Peak NCX current density.** Peak Na<sup>+</sup>-Ca<sup>2+</sup> exchange (NCX) current density at fixed Ca<sup>2+</sup> and Na<sup>+</sup> concentrations was unchanged in left ventricle (LV) and right ventricle (RV) of control (Ctrl) and plakophilin-2 conditional knockout (PKP2cKO) samples. Voltage clamp protocol in the detailed Methods section. Black bars correspond to Ctrl hearts and red bars correspond to PKP2cKO (Mean±standard error of the mean; SEM). Number of recorded cells indicated within each bar. Cells obtained from 3 control and 4 PKP2cKO animals.



Gene	Mean	Log2FC	Padj
<i>Nrn1</i>	214.2	-1.46	1.0e-15
<i>Cnksr1</i>	135.1	-1.12	1.0e-15
<i>Ptgds</i>	2135.2	-1.09	1.0e-15
<i>Acta1</i>	4707.7	-1.02	7.2e-13
<i>Rp1</i>	109	1.68	1.0e-15
<i>Mybphl</i>	415.3	1.59	1.0e-15
<i>Sln</i>	665.9	1.52	1.0e-15
<i>Cacna1h</i>	442.8	1.19	1.0e-15
<i>Sbk2</i>	293.8	1.28	1.0e-15
<i>Aqp4</i>	196.3	1.33	1.0e-15
<i>Tmem163</i>	72.8	1.45	1.0e-15
<i>Slit2</i>	311.2	1.02	1.0e-15
<i>H19</i>	1004.5	1.18	1.0e-15
<i>Lmntd1</i>	84.8	1.28	1.0e-15
<i>Retn1a</i>	103.2	1.21	1.0e-15
<i>Wif1</i>	118.7	1.25	1.0e-15
<i>Aldob</i>	230.5	1.03	1.0e-15
<i>Vsig4</i>	90.8	1.17	1.0e-15
<i>Myl4</i>	3850.4	1.12	1.0e-15
<i>Ptgfr</i>	136.8	1.04	5.9e-14
<i>Drd2</i>	124.4	1.03	8.3e-14

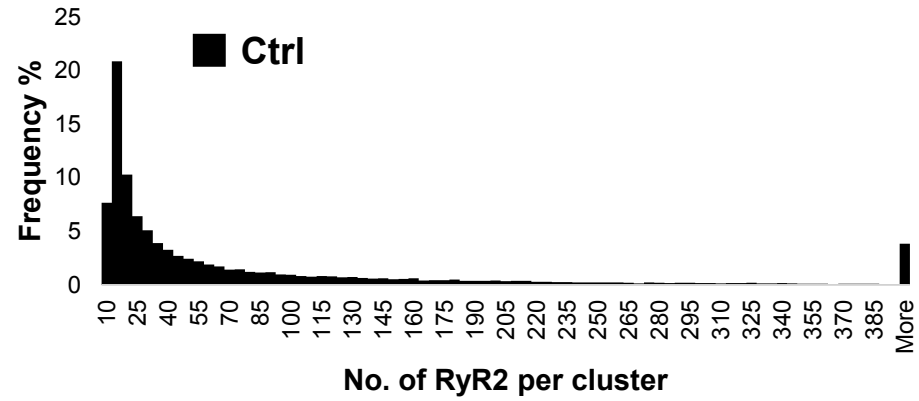


Gene	Mean	Log2FC	Padj
<i>Cenpf</i>	963.4	1.19	1.0e-15
<i>Nrn1</i>	229.7	-1.67	1.0e-15
<i>Igf2</i>	864.1	1.11	1.0e-15
<i>Slit2</i>	315.7	1.39	1.0e-15
<i>Aqp4</i>	179.8	1.44	1.0e-15
<i>Cntn2</i>	205.6	1.20	1.0e-15
<i>Ubxn10</i>	173.5	1.10	1.0e-15
<i>Wif1</i>	106.7	1.06	3.0e-14
<i>Cnksr1</i>	151.0	-1.02	3.5e-14

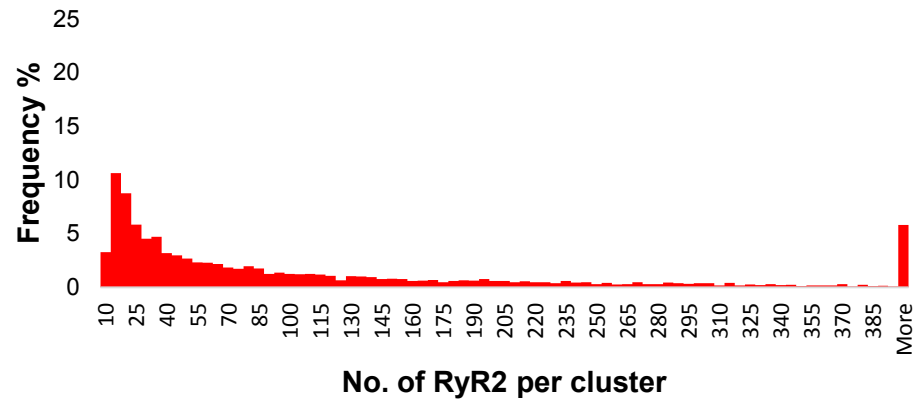
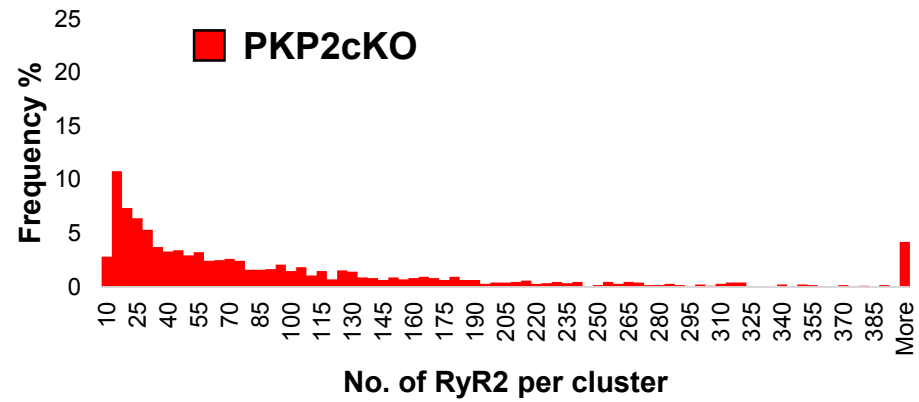
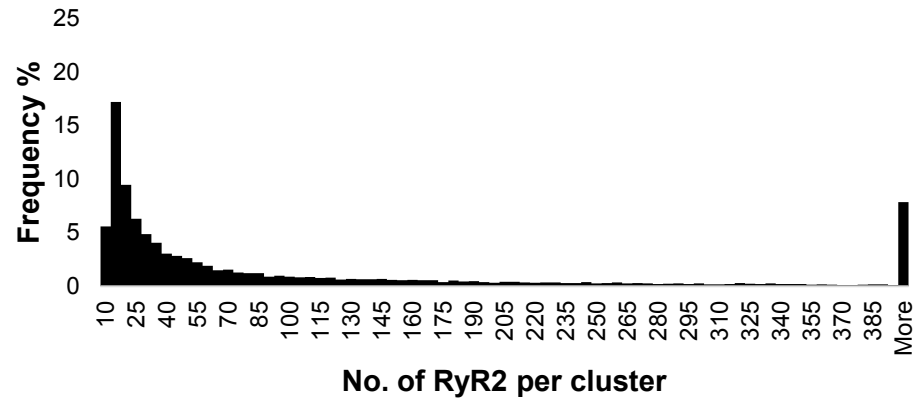
Supplemental figure V

**Figure V. Right versus left transcriptomic analysis in control and PKP2cKO mice. A:** Top: Volcano plot of upregulated or down-regulated transcripts in the right ventricle (RV) (relative to left ventricle; LV) of control hearts. Red dots correspond to transcripts with  $\text{Log}_2\text{FC} > \pm 1.0$  and  $-\log_{10}(\text{FDR}) > 2$  ( $\text{padj} < 0.01$ ); Blue dots:  $\text{Log}_2\text{FC}$  between 0 and  $\pm 1.0$  and  $-\log_{10}(\text{FDR}) > 2$ ; Grey dots: transcripts with  $\log_{10}(\text{FDR}) < 2$ . Transcripts corresponding to the red dots are listed in the bottom panel.  $n=5$  mice. FDR: false discovery rate. **B:** Same as **A** but in this case, samples were obtained from 5 plakophilin-2 conditional knockout (PKP2cKO) mice 14 days post-tamoxifen (TAM). Only nine transcripts in the PKP2cKO group met criteria for significance and magnitude of differential, and four of them were also differentially expressed in the control (Ctrl), as examined by paired comparisons, analyzed by paired  $t$ -tests corrected by the Benjamini and Hochberg method. Consistent with the fact that no major differences in transcript abundance were detected between groups, a principal component analysis (PCA) did not produce a defined segregation of experimental sets into separate clusters. In other words, the PCA predicted that there was insufficient variability between samples to discriminate them statistically, in agreement with the results obtained through the paired  $t$ -test comparisons. Complete datasets can be found in the accompanying Table I and Table II in the online-only supplemental data section. ribonucleic acid sequencing (RNAseq) data analysis carried out using the DESeq2 package (<https://bioconductor.org/packages/release/bioc/html/DESeq2.html>).

**LV**



**RV**



Supplemental figure VI

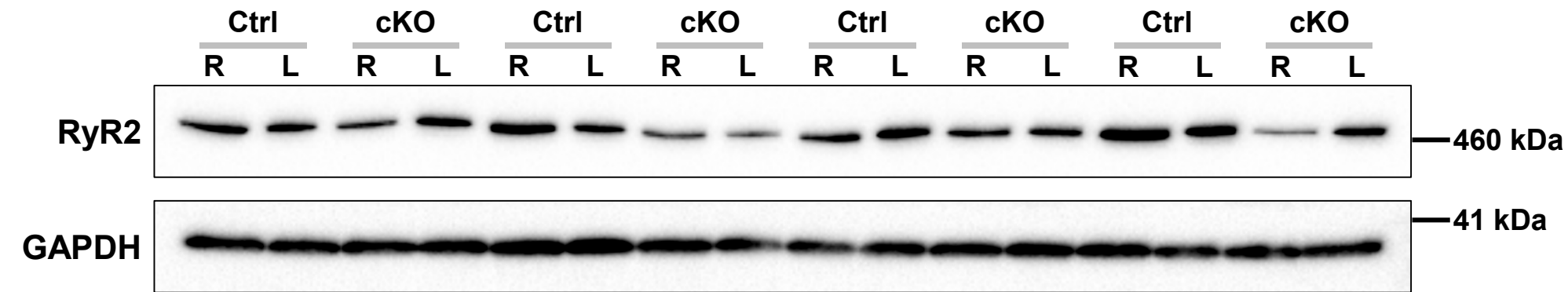
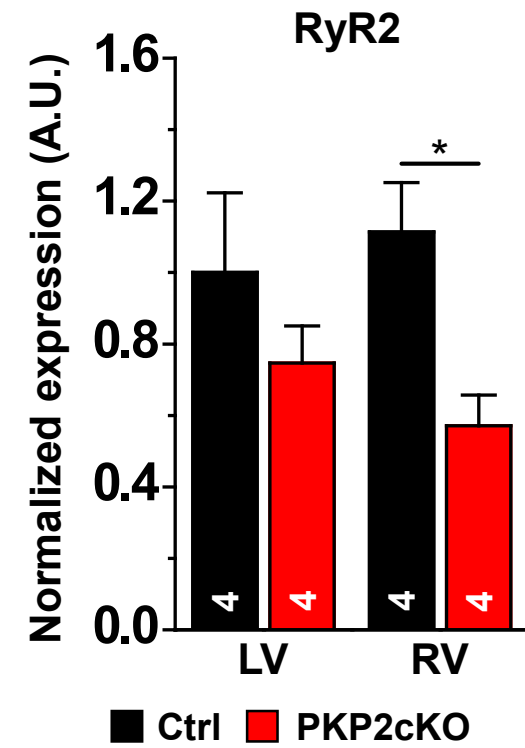


**Figure VI. Distribution histogram of fraction of the total number of RyRs (Frequency %) as a function of the number (No.) of ryanodine receptor 2 (RyR2) per cluster in control (Ctrl; black) and plakophilin-2 conditional knockout (PKP2cKO) left and right ventricles (red). The Ctrl group shows a larger peak in the 10-25 range, while the PKP2cKO group shows a broader distribution. Values specified in Supplemental Figure VII.**

		Median No. RyR2 per cluster	Mean No. RyR2 per cluster	Cluster size (nm <sup>2</sup> )		
LV	Ctrl	30	89	108,438	±	1,261
	<b>PKP2cKO</b>	57	107 ***	37,387	±	725 ***
RV	Ctrl	40	130 †††	129,565	±	2,155 †††
	<b>PKP2cKO</b>	58	119 *** †††	42,659	±	619 *** †††

Supplemental figure VII

**Figure VII. Median and mean number of ryanodine receptor 2 (RyR2) molecules per cluster, and average cluster size  $\pm$  standard error of the mean (in nm<sup>2</sup>) in each condition.** Parameters were calculated using Density-Based Spatial Clustering of Applications with Noise (DBSCAN) analysis. Total number of clusters analyzed (clusters that have at least 10 RyRs):  $n=32738$  RyR2 clusters from left ventricular (LV) myocytes and 16595 clusters from right ventricular (RV) myocytes from control; 1666 LV and 4396 RV clusters from PKP2cKO mice. Two-way repeated measures analysis of variance (ANOVA)-Bonferroni, \*\*\* $p<0.001$  vs. control, ††† $p<0.001$  vs. LV.

**A****B**

**Figure VIII. Ryanodine receptor 2 (RyR2) abundance in samples used to calculate [<sup>3</sup>H]Ryanodine binding. A:** The term “Ctrl” refers to samples from control animals. “cKO” refers to samples obtained from plakophilin-2 conditional knockout (PKP2cKO) animals, 14 days post-tamoxifen (TAM). R: right ventricle, L: left ventricle. **B:** Average normalized expression.  $n=4$  for each group. Each “n” is a pool of samples obtained from 3 hearts. LV: left ventricle. RV: right ventricle.  $*p<0.05$  vs. control. Two-way repeated measures analysis of variance (ANOVA)-Bonferroni test.

**A**

Accession Number	Species		Sequence	
Q92736	Human	2800	LYNRTRRI <b>SQ</b> <b>T</b> SQV <b>SV</b> DAAHG	2820
P30957	Rabbit	2801	LYNRTRRI <b>SQ</b> <b>T</b> SQV <b>SV</b> DAAHG	2821
E9Q401	Mouse	2799	LYNRTRRI <b>SQ</b> <b>T</b> SQV <b>S</b> I DAAHG	2819
B0LPN4	Rat	2790	LYNRTRRI <b>SQ</b> <b>T</b> SQV <b>S</b> I DAAHG	2810
*	Pig	2801	LYNRTRRI <b>SQ</b> <b>T</b> SQV <b>SV</b> DAAHG	2821

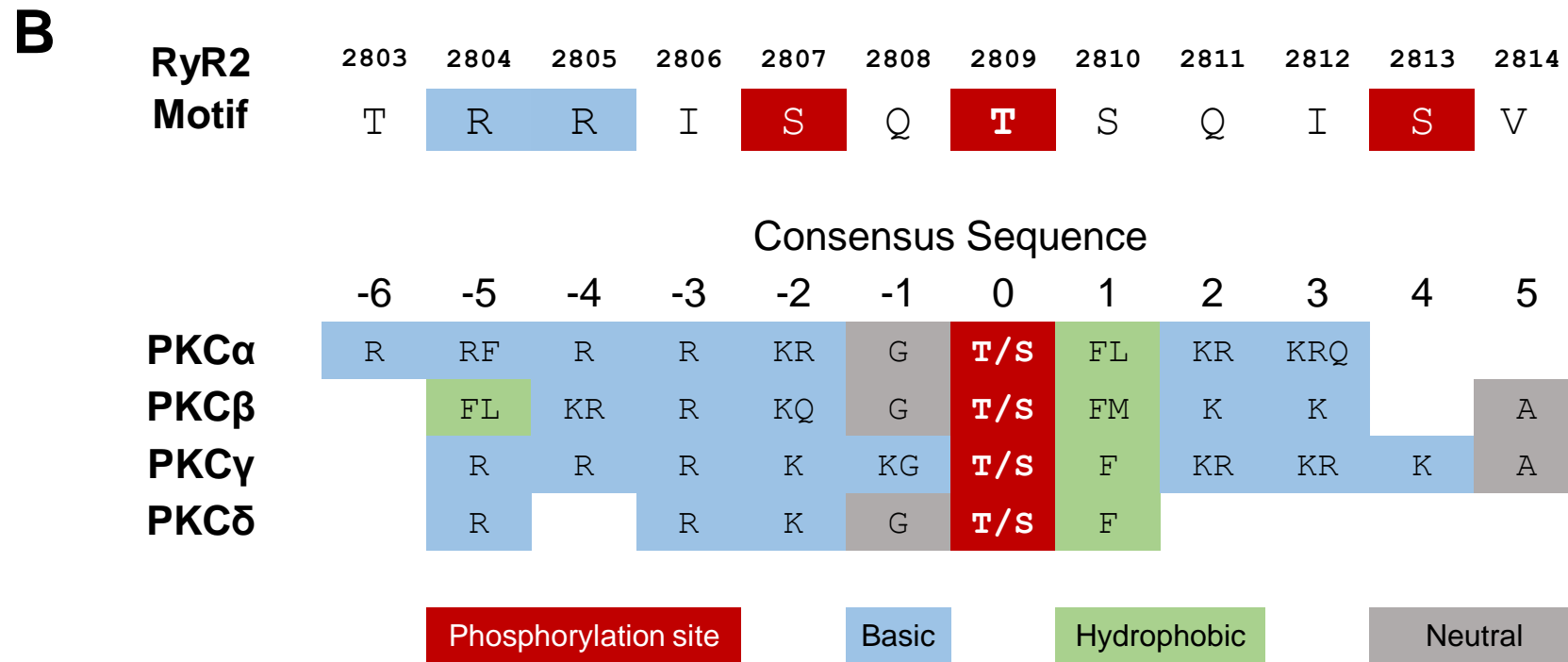
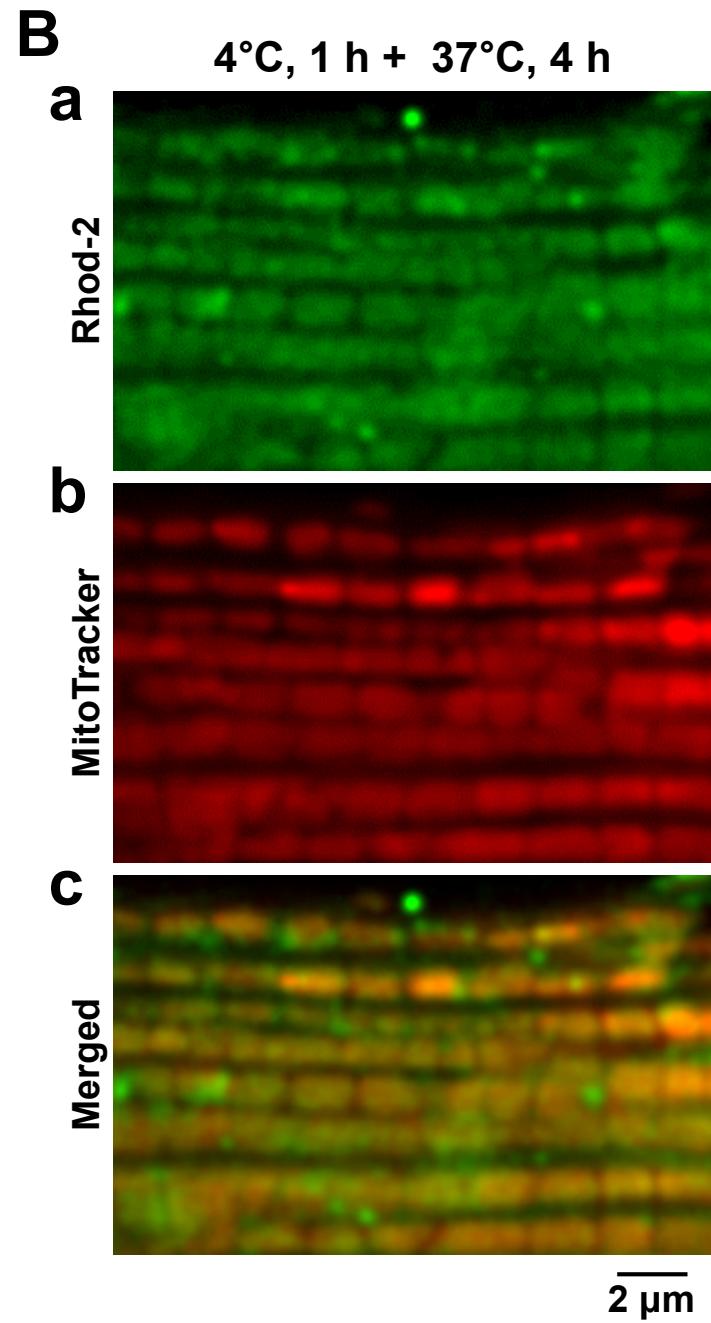
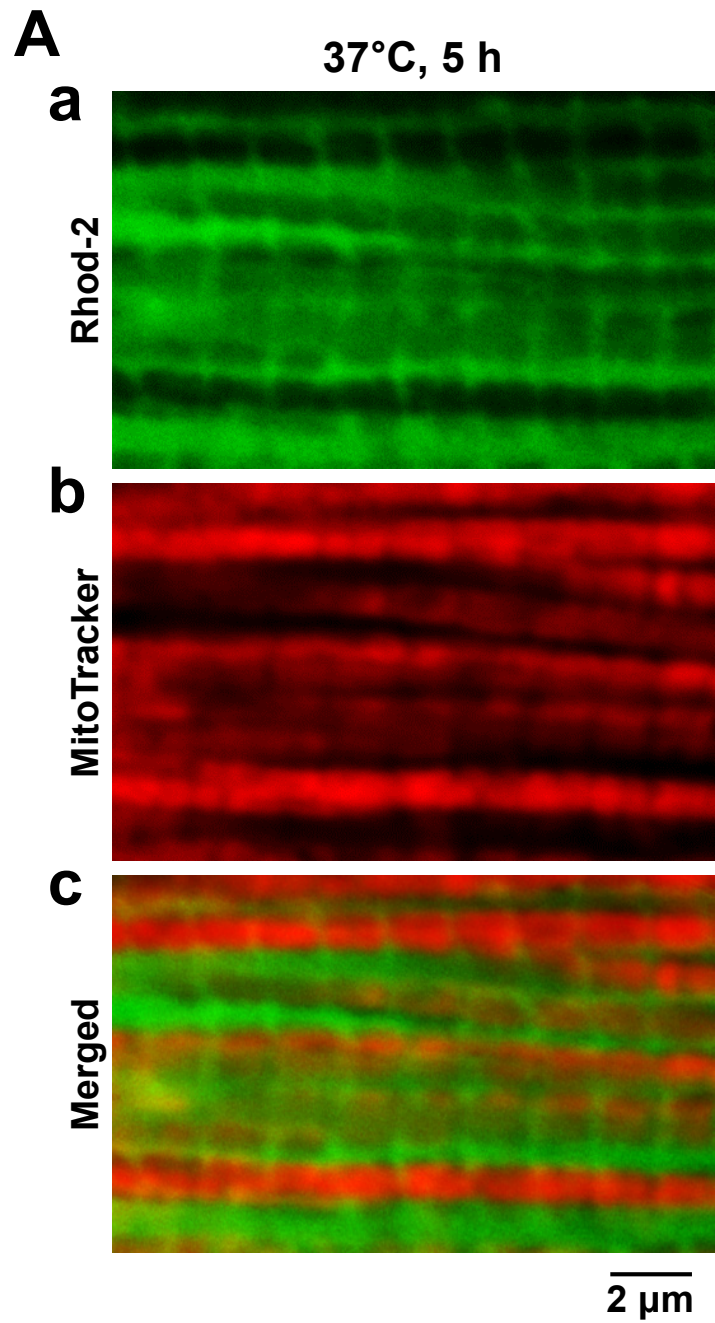


**Figure IX. Alignment of the phosphorylation hotspot of RyR2 and the potential protein kinase C (PKC) target at Thr2809.** A: Alignment of the “phosphorylation hotspot” of ryanodine receptor 2 (RyR2) for the species noted in the left. Accession numbers from Uniprot ([www.uniprot.org](http://www.uniprot.org)). The pig sequence was reconstructed from previous publications<sup>28</sup>. Flanking numbers correspond to the RyR2 sequence number for each species. The red “T” marks the preservation of the threonine residue. Serines 2807 and 2813, known as kinase substrates, are noted in green. B: RyR2 sequence as a potential substrate for PKC phosphorylation, based on the consensus motifs of the various PKC isoforms.

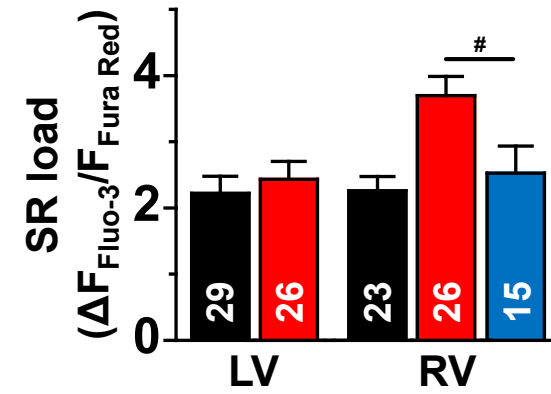
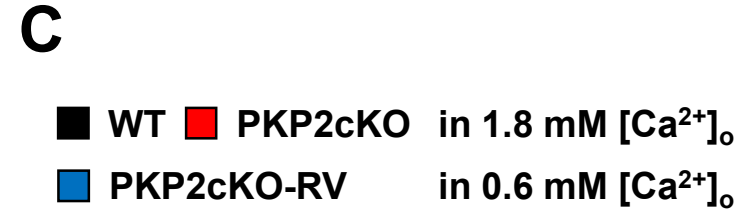
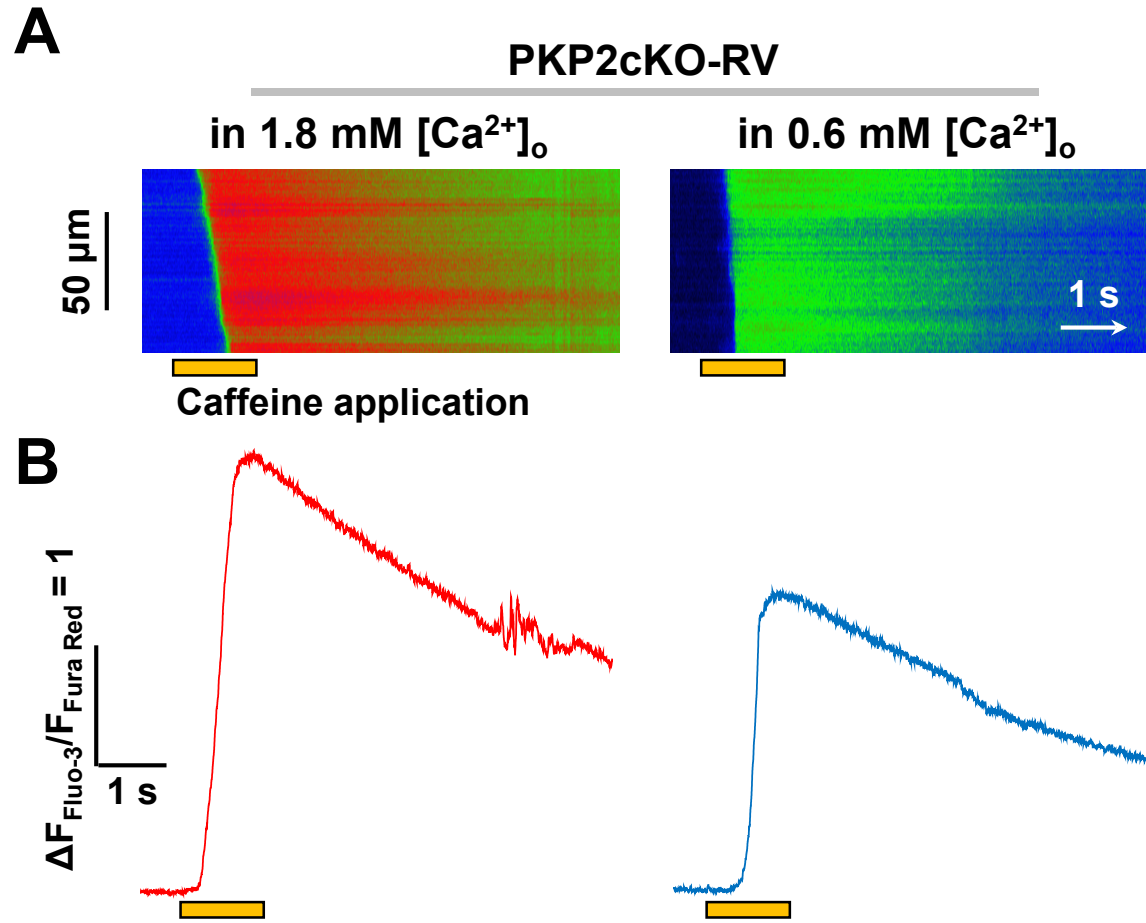




**Figure X. Ca<sup>2+</sup> content in the intracellular compartments.** **A:** Confocal line-scan images (1.43 ms/line) recorded from permeabilized myocytes isolated from the left ventricle (LV) or the right ventricle (RV) free wall of either control (Ctrl) or plakophilin-2 conditional knockout (PKP2cKO) mice 14 days post- tamoxifen (TAM). In this and other panels, the pulse of caffeine (10 mM) is indicated by the orange bar at the bottom of the image. **B:** Time course and amplitude of the change in fluorescence during and immediately following the caffeine pulse. Notice the larger amplitude of the transient recorded from PKP2cKO RV myocytes. Cumulative data are shown in **C**. Number of experiments noted in the bar graphs. Cells originated from three different mice in each group (Ctrl or PKP2cKO). \*\*\* $p < 0.001$  vs. control, † $p < 0.05$  vs. LV. Two-way repeated measures analysis of variance (ANOVA)-Bonferroni test.

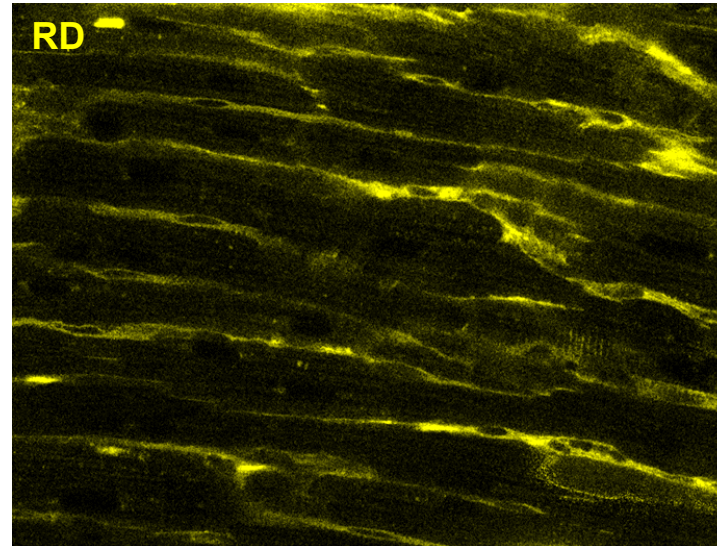
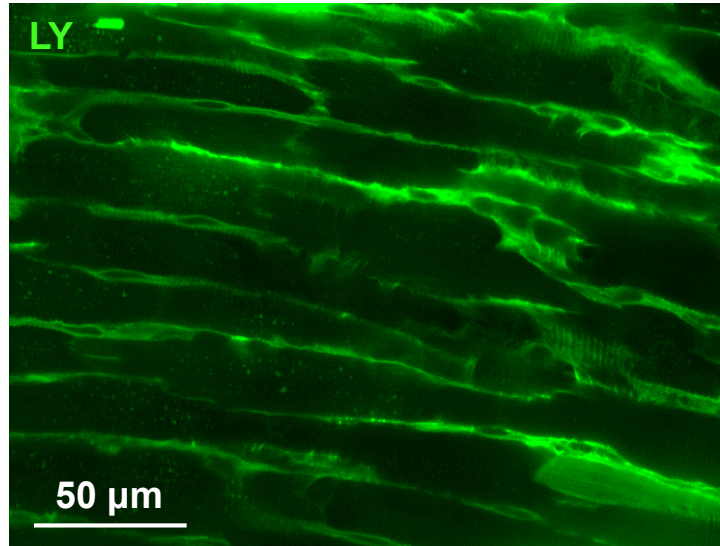
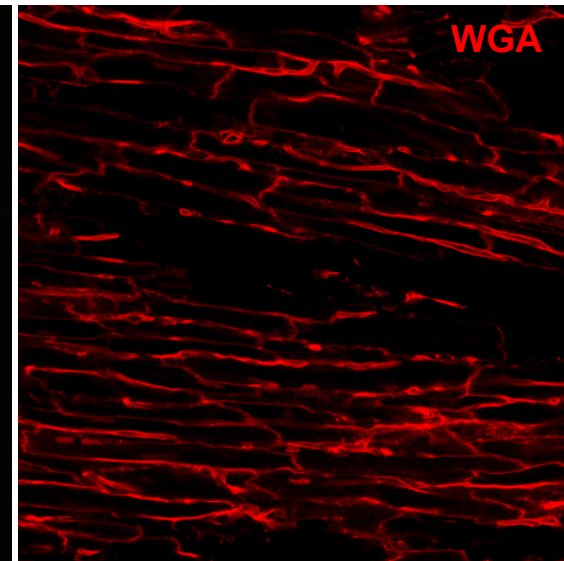
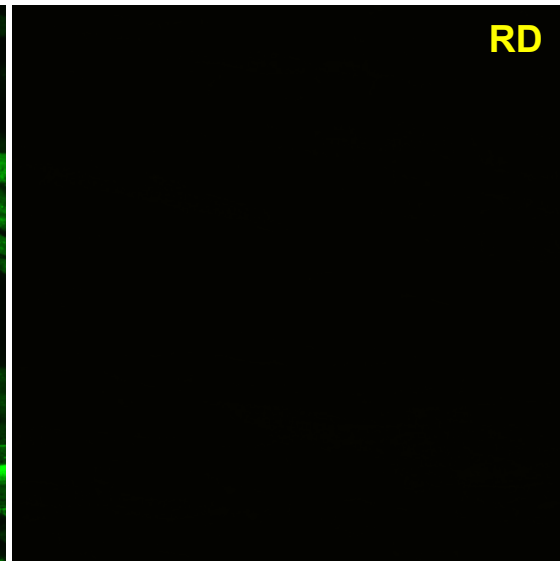
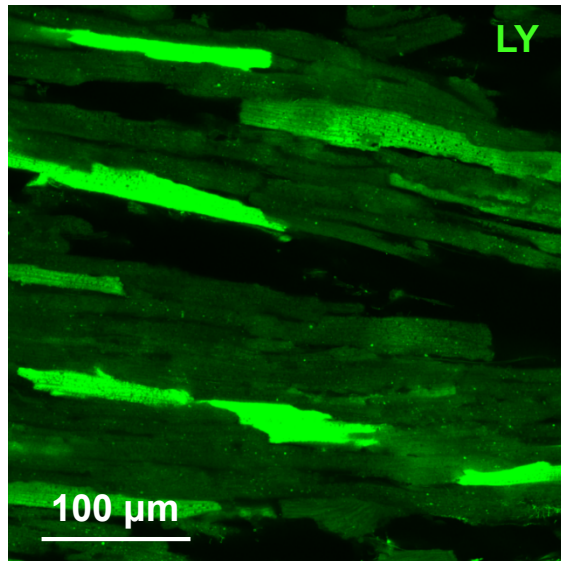


**Figure XI. Temperature-dependent loading of Rhod-2 into mitochondria of isolated adult cardiomyocytes.** **A:** Ventricular myocytes were loaded with 2  $\mu\text{M}$  Rhod-2 AM in 37°C for 5 h and then labeled with 200 nM MitoTracker Deep Red FM (fluorescent molecules) for additional 10 min (37°C). Rhod-2 (**Aa**) and MitoTracker (**Ab**) fluorescence signals visualized with confocal fluorescence imaging. Merged image (**Ac**) of the Rhod-2 and MitoTracker signals showed that, when loading at warm temperatures, Rhod-2 was predominantly localized to the cytoplasm rather than in the mitochondria. **B:** Ventricular myocytes were loaded with 2  $\mu\text{M}$  Rhod-2 AM in 4°C for 1 h and followed by 37°C for 4 h and then labeled with 200 nM MitoTracker Deep Red FM for additional 10 min (37°C). Rhod-2 (**Ba**) and MitoTracker (**Bb**) fluorescence signals visualized with confocal fluorescence imaging. Merged image (**Bc**) of the Rhod-2 and MitoTracker signals showed that Rhod-2 was selectively loaded to the mitochondria. This latter protocol was used for the experiments reported in Figure 5 of the manuscript.



Supplemental figure XII

**Figure XII. SR load as a function of extracellular  $\text{Ca}^{2+}$  in PKP2cKO-RV myocytes.** Panel **A**: time-space plots showing  $\text{Ca}^{2+}$  transients elicited by a pulse of caffeine (same protocol as in Figure 5A of the main manuscript). Time course in Panel **B**. Data obtained from a plakophilin-2 conditional knockout (PKP2cKO)-right ventricular (RV) cell recorded at 1.8 mM  $[\text{Ca}^{2+}]_o$  (left) and from a separate PKP2cKO-RV cell recorded at 0.6 mM  $[\text{Ca}^{2+}]_o$ . As shown by the cumulative data in panel **C**, decreasing  $[\text{Ca}^{2+}]_o$  to 0.6 mM equalized the amplitude of the caffeine-induced transient to a level comparable to that observed in control or in PKP2cKO-left ventricle (LV) at  $[\text{Ca}^{2+}]_o$  1.8 mM. Data for RV and LV controls and PKP2cKO are reproduced from Figure 5A for comparison. For the PKP2cKO-RV at 0.6 mM  $[\text{Ca}^{2+}]_o$ ,  $n=15$  from 3 mice.  $\#p<0.05$  vs. PKP2cKO RV in 1.8  $[\text{Ca}^{2+}]_o$ . Two-way repeated measures analysis of variance (ANOVA)-Bonferroni test.

**A****Dye Unwashed****B**

Supplemental figure XIII

**Figure XIII. Dye uptake assay in intact heart. A:** A murine adult heart was Langendorff-perfused with a solution containing Lucifer Yellow (LY) and Rhodamine Dextran (RD) and then immediately imaged by confocal microscopy. Notice that both dyes are abundantly localized to the interstitial/capillary space. In contrast, **B** shows a confocal image of a heart loaded with LY, RD and Wheat Germ Agglutinin (WGA), subsequently washed with dye-free solution and then fixed in paraformaldehyde (PFA) overnight. Note that Rhodamine Dextran (average molecular weight ~10,000) was not loaded in the cells and was removed by the wash, indicating that Lucifer Yellow did not enter the cells through the damaged sarcolemma.

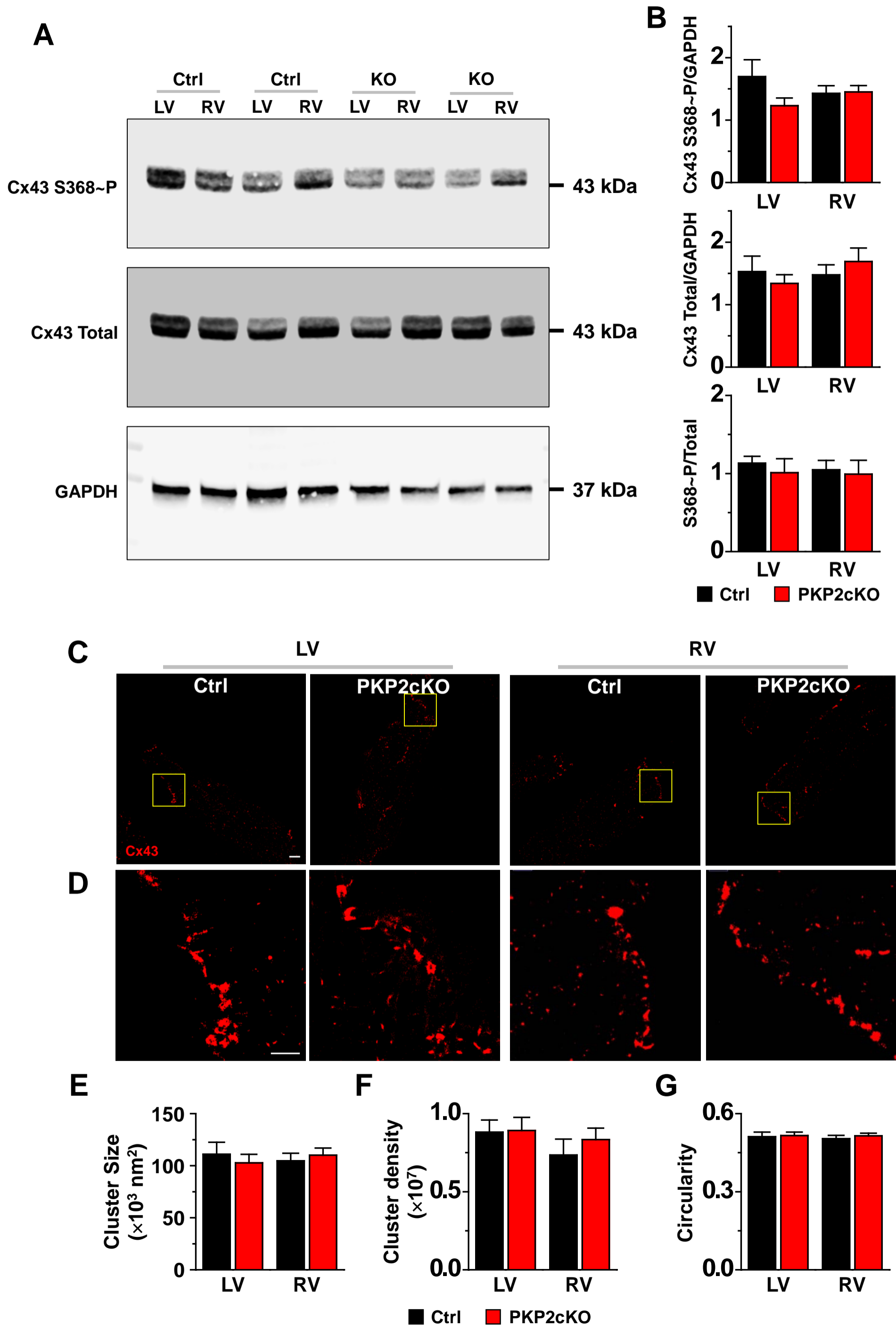
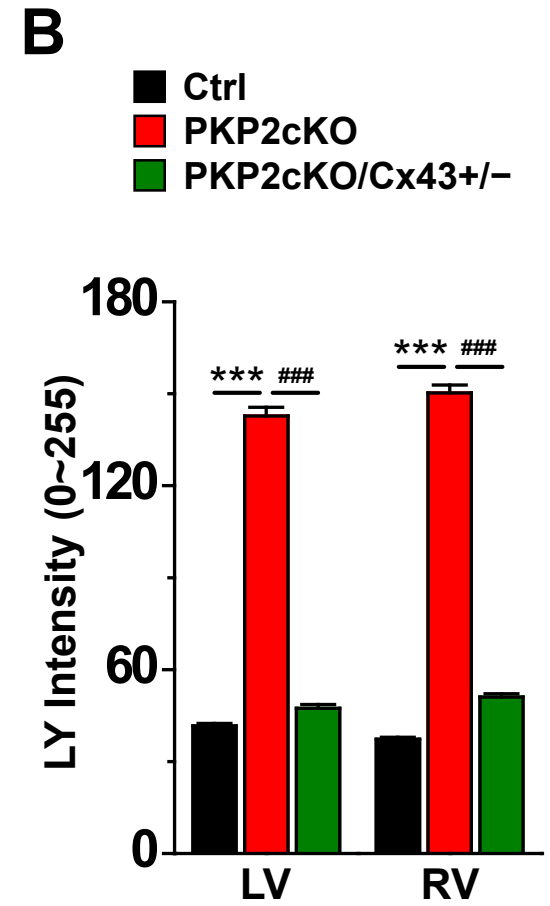
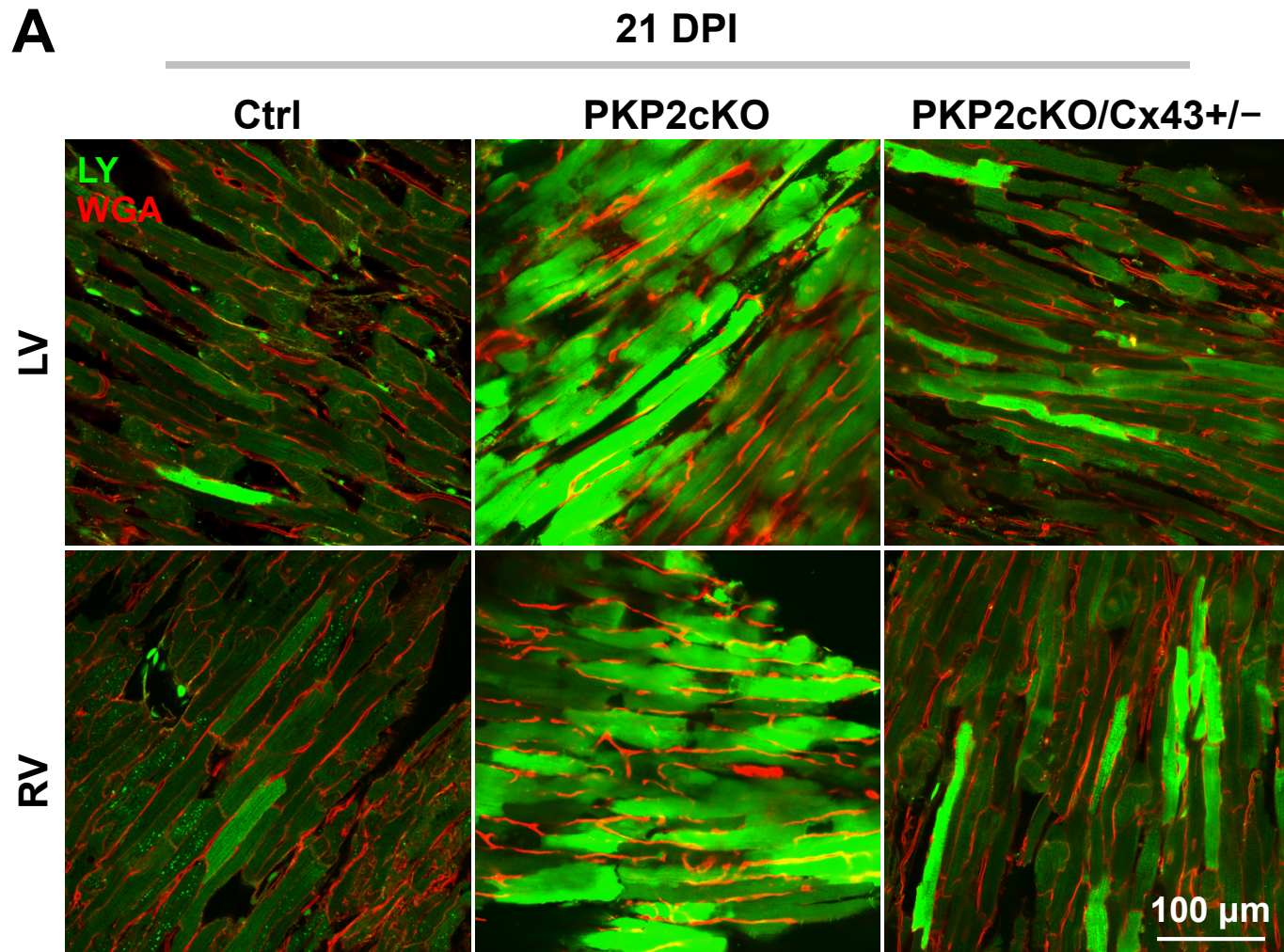




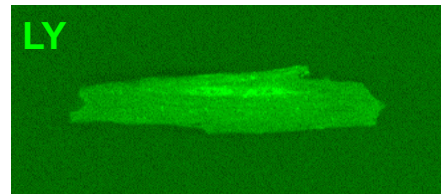
**Figure XIV. Abundance and localization of Cx43 is unaltered in PKP2cKO mice at 14 days post-tamoxifen (TAM).** Western blot examples are shown in the upper left panel (**A**), and the results of densitometry analysis are shown in the bar graphs (**B**). Methods in the “Detailed Methods” section. Number of hearts: 9 and 8 for control (Ctrl) and plakophilin-2 conditional knockout (PKP2cKO), respectively. GAPDH: glyceraldehyde 3-phosphate dehydrogenase. **C**: Stochastic optical reconstruction microscopy (STORM)-acquired images of Cx43 in single myocytes dissociated from left ventricle (LV) or right ventricle (RV) of Ctrl or PKP2cKO mice 14 days post-TAM (scale bar 5  $\mu$ m) . **D**: Enlargement of the yellow-boxed areas in **C** showing part of the cell ends (scale bar in insets, 2  $\mu$ m). **E**, **F** and **G**: Average size, cluster density and cluster circularity (1.0 indicates perfect circle) of Cx43 clusters in control and PKP2cKO myocytes measured at the cell end. Control:  $n=15$  LV cells; and 14 RV cells from 2 mice. PKP2cKO:  $n=14$  LV cells; and 17 RV cells from 2 mice. The results show no differences between the groups when examined by two-way repeated measures analysis of variance (ANOVA)-Bonferroni.



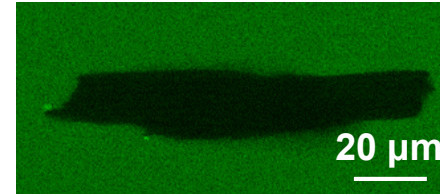
Supplemental figure XV

**Figure XV. Membrane permeability to Lucifer Yellow and effect of Cx43 expression in plakophilin-2 conditional knockout (PKP2cKO) hearts 21 days post-tamoxifen (TAM).** **A:** Confocal images collected from the epicardial phase of either the left ventricular (LV) or the right ventricular (RV) free wall of hearts harvested from control (Ctrl), PKP2cKO mice 21 days post-TAM (PKP2cKO) or a conditional knockout of PKP2 also heterozygous conditional for Cx43 (i.e., PKP2cKO/Cx43+/-), also at 21 days post-TAM. Images were obtained after a 30-min perfusion with 1 mg/mL Lucifer Yellow (LY; MW 457; green), 1 mg/mL Rhodamine Dextran (RD; MW ~10,000) and 0.04 mg/mL Wheat Germ Agglutinin (WGA; red) in 10 nM free [Ca<sup>2+</sup>] solution (see “Methods” for further details). Image fields were chosen at random and the intensity of the LY fluorescence (in a scale 0-225) was measured within regions of interest (ROIs) that excluded areas voided of cells. MW: molecular weight. **B:** Average LY intensity measured from cells in the following groups: Control (Ctrl; black bars; *n*=327 LV cells, 395 RV cells from 2 mice), PKP2cKO (red bars; *n*=348 LV cells, 415 RV cells from 2 mice) and PKP2cKO/Cx43+/- (green bars; *n*=690 LV cells, 291 RV cells from 2 mice). \*\*\**p*<0.001 vs. control; ###*p*<0.001 vs. PKP2cKO. Two way repeated measures analysis of variance (ANOVA)-Bonferroni.

Ctrl ventricular myocytes in Ca<sup>2+</sup>-free (2 mM EGTA) solution



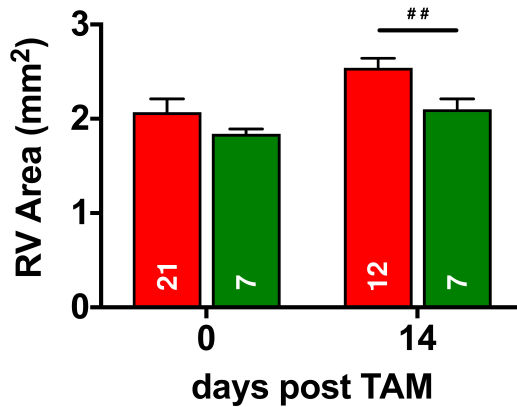
w/o TAT-Gap19



w/ TAT-Gap19

Supplemental figure XVI

**Figure XVI. Effect of TAT-Gap19 on cell permeability to Lucifer Yellow (LY).** Left: single myocyte maintained in  $\text{Ca}^{2+}$  -free solution and exposed to LY. Notice fluorescence emitted from the intracellular space. Right: Same experiment but in the presence of transactivator of transcription (TAT)-Gap19. Notice the absence of fluorescence emission, likely consequent to inhibition of Cx43 hemichannel activity.



Supplemental figure XVII

**Figure XVII. Echocardiographic measurements.** Echocardiographic measurements of right ventricular area of PKP2cKO/Cx43<sup>+/-</sup> mice, compared to plakophilin-2 conditional knockout (PKP2cKO) (the latter dataset also reported in<sup>2</sup> numbers in the bars indicate number of animals tested). RV: right ventricle; TAM: tamoxifen. <sup>##</sup> $p < 0.01$  by unpaired  $t$ -test. Only one comparison between two variables (RV Area PKP2cKO vs. PKP2cKO/Cx43<sup>+/-</sup> at 14 days post-TAM).

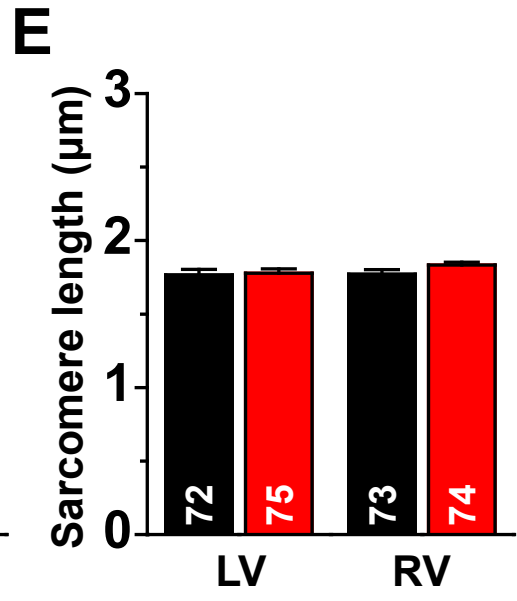
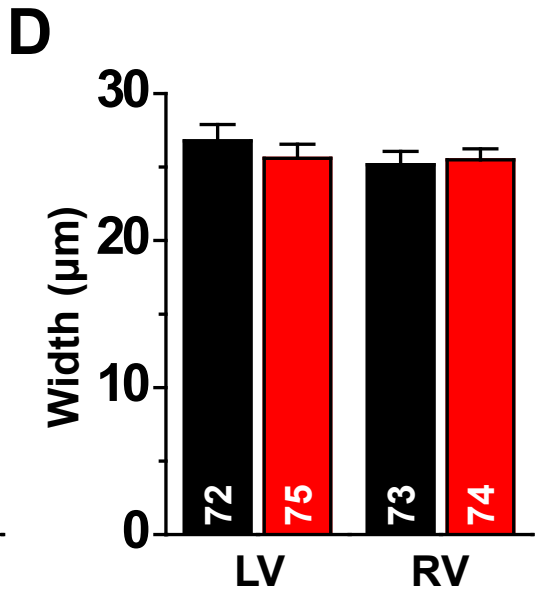
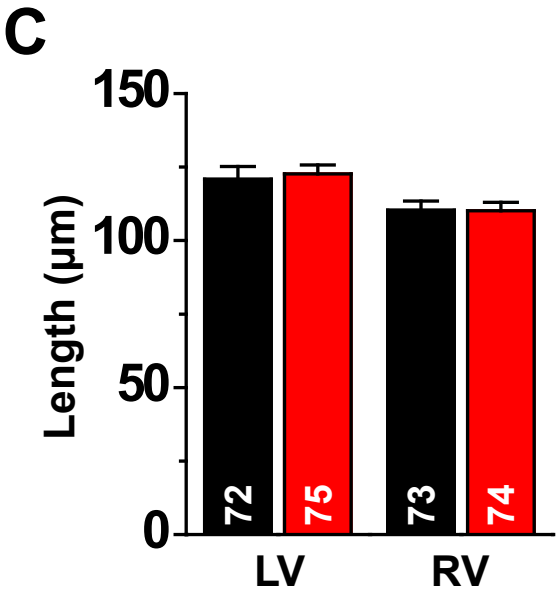
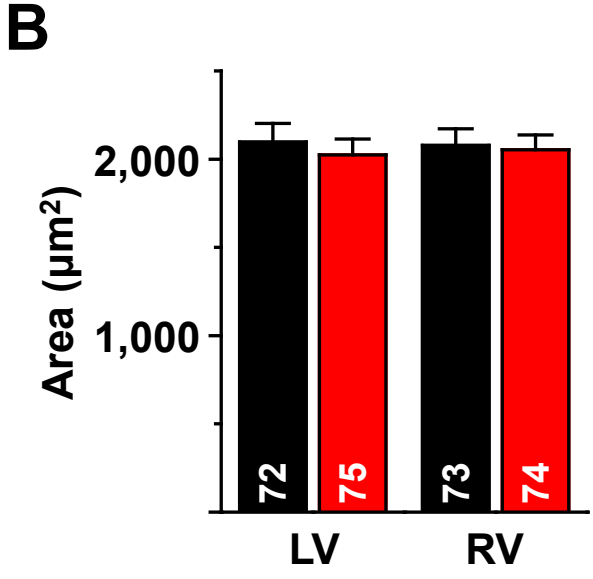
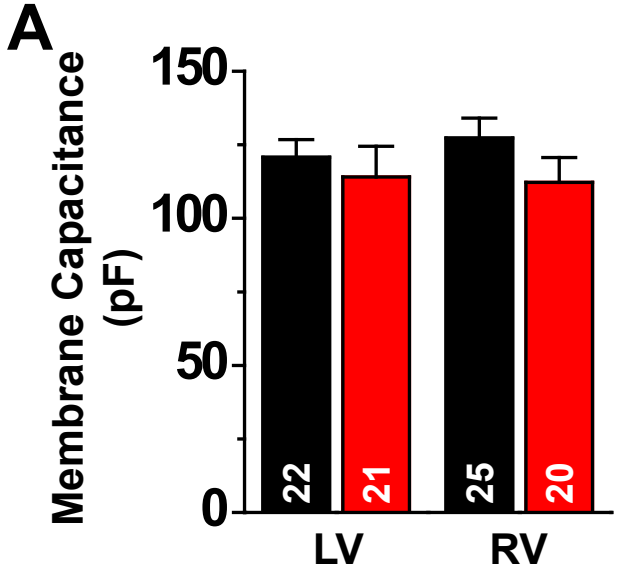




**Figure XVIII. Analysis of cell morphology.** In all panels, black and red bars correspond to data from control and plakophilin-2 conditional knockout (PKP2cKO) myocytes, respectively. **A:** Isolated cells were recorded to measure cell capacitance by the procedure detailed in Methods. Separately, cell morphology was determined by light microscopy to measure surface area (**B**), cell length and width (**C, D**) and sarcomere length (**E**). The results show no differences between the groups. Numbers in the bars indicate *n* values of cells tested. 4 mice were used for each group.



**Figure XIX. Analysis of phosphoPKC-T638/641 clustering using single molecule-localization microscopy single molecule localization microscopy (SMLM) by stochastic optical reconstruction microscopy (STORM)** **A:** STORM-acquired images of phosphoPKC-T638/641 (in green; pPKC) and N-cadherin (in red; Ncadh) in single myocytes dissociated from left ventricle (LV) or right ventricle (RV) of control (Ctrl) or plakophilin-2 conditional knockout (PKP2cKO) mice 14 days post-TAM (scale bar 5  $\mu$ m). TAM: tamoxifen. **B:** Enlargement of the yellow-boxed areas in A showing the cell ends (scale bar in insets, 2  $\mu$ m). **C** and **D:** Average cluster size and cluster density of phosphoPKC clusters in control and PKP2cKO myocytes measured at the cell ends. **E:** Distances from phosphoPKC clusters to the cell end marked as N-cadherin (measured in nm).  $n=692$  clusters from 27 LV cells; 815 clusters from 28 RV cells, from 3 mice. PKP2cKO:  $n=596$  clusters from 33 LV cells; 524 clusters from 31 RV cells, from 3 mice. Statistical significance by two-way repeated measures analysis of variance (ANOVA)-Bonferroni, \* $p<0.05$  vs. control, † $p<0.05$  vs. LV, \*\*\* $p<0.001$  vs. control, and ††† $p<0.001$  vs. LV.

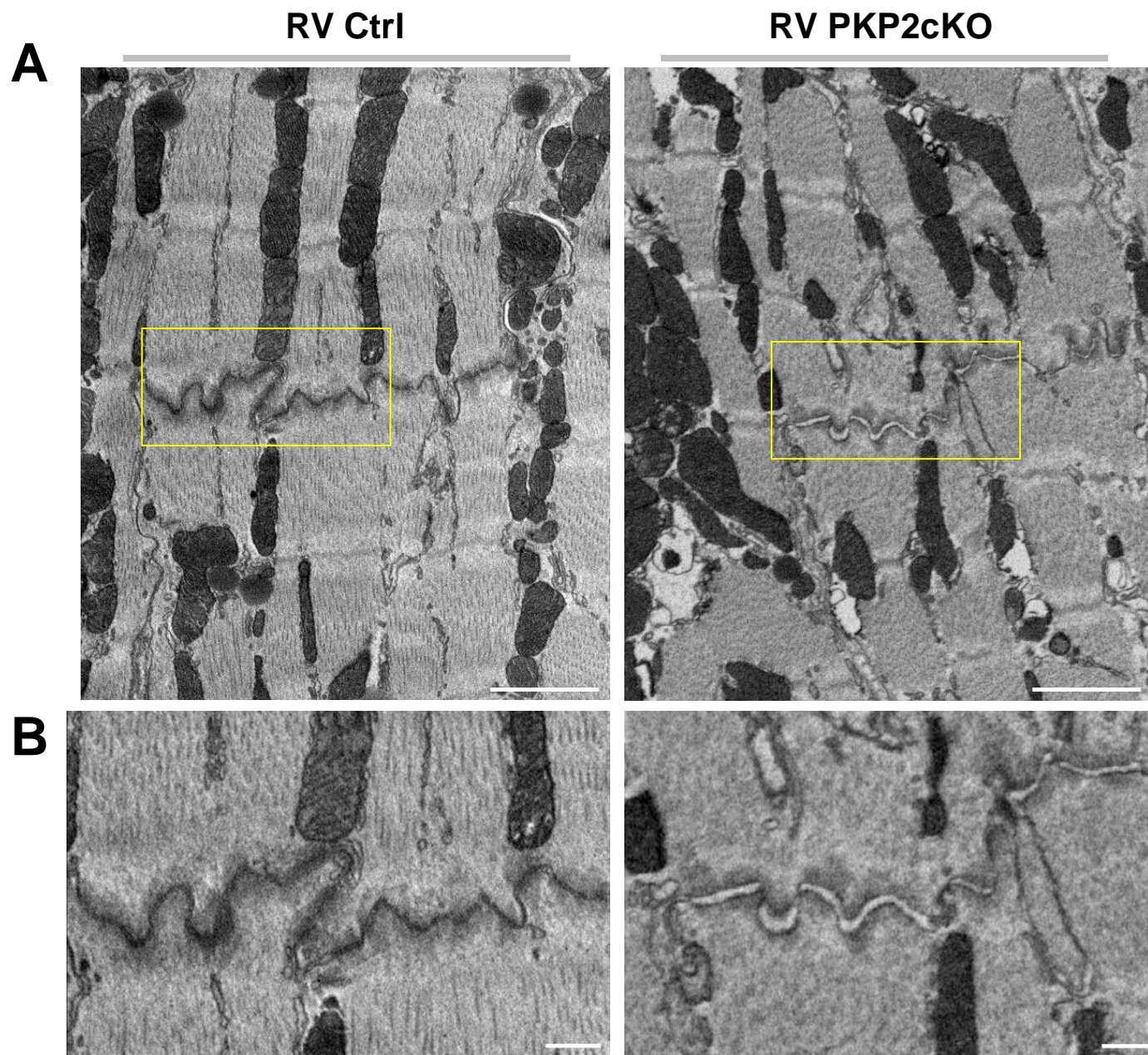
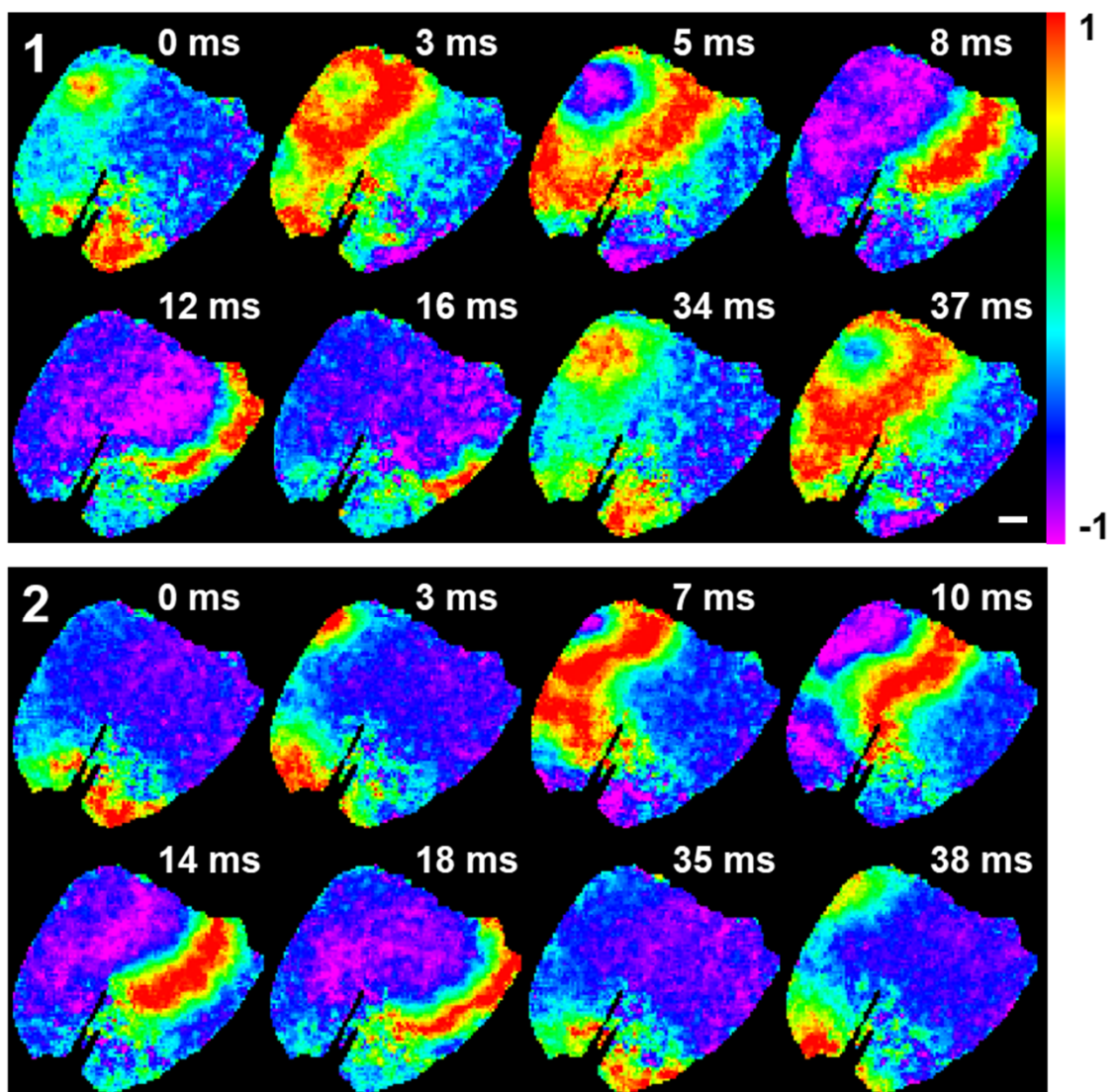
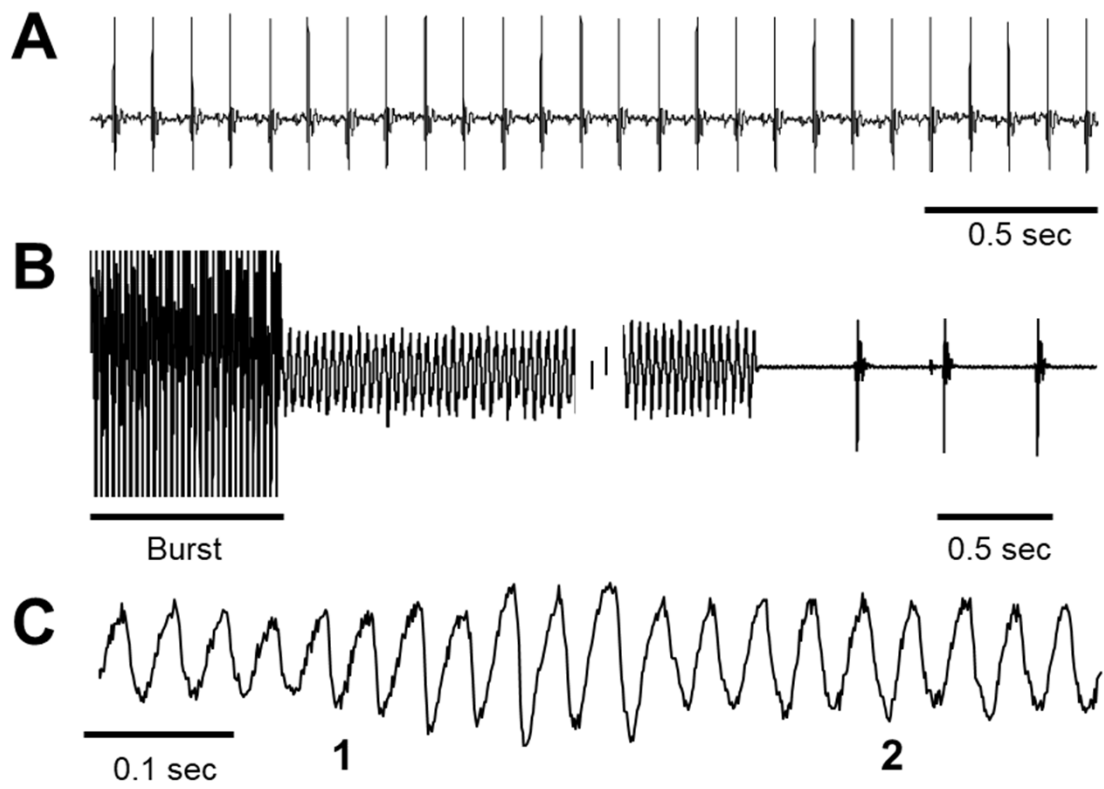


**Figure XX. Intercalated disc ultrastructure.** **A:** Single frame of a complete focused ion beam-scanning electron microscopy (FIB-SEM)-acquired set showing the ultrastructure of the intercalated disc from a control (Ctrl; left panel) and a plakophilin-2 conditional knockout (PKP2cKO; right panel) right ventricle (RV) tissue, 14 days post-tamoxifen (TAM). Scale bar: 2  $\mu\text{m}$ . Enlarged images (yellow-boxed areas) are shown in **B** (Scale bar: 0.5  $\mu\text{m}$ ). Notice increased intercellular distance in the sample from PKP2cKO-RV. A complete 3D volume is presented in supplemental videos 1 and 2.



Supplemental figure XXI

**Figure XXI. High-resolution optical mapping of electrical activation in Langendorff-perfused hearts.** **A:** Volume-conducted electrocardiogram (ECG) showing sinus rhythm. **B:** Volume-conducted ECG obtained after burst stimulation of the right ventricle (RV) free wall. Notice run of ventricular tachycardia after burst, and spontaneous self-termination. **C-top:** Optical pseudo-ECG obtained from the RV free wall during a triggered polymorphic ventricular tachycardia. **C-Bottom:** dF/dt maps showing propagation of the electrical wavefront at two time windows (1 and 2 as marked in C-top). Data were acquired after 1 minute of perfusion with a solution containing 100 nM Isoproterenol. A total of 4 hearts were tested for each group. Ventricular arrhythmias were recorded in all 4 plakophilin-2 conditional knockout (PKP2cKO) hearts and in none of the controls. Scale bar: 1 mm. Experimental protocol detailed in the “Methods” section.

## REFERENCES

1. Liao Y, Day KH, Damon DN and Duling BR. Endothelial cell-specific knockout of connexin 43 causes hypotension and bradycardia in mice. *Proc Natl Acad Sci U S A*. 2001;98:9989-9994.
2. Cerrone M, Montnach J, Lin X, Zhao YT, Zhang M, Agullo-Pascual E, Leo-Macias A, Alvarado FJ, Dolgalev I, Karathanos TV, Malkani K, Van Opbergen CJM, van Bavel JJA, Yang HQ, Vasquez C, Tester D, Fowler S, Liang F, Rothenberg E, Heguy A, Morley GE, Coetzee WA, Trayanova NA, Ackerman MJ, van Veen TAB, Valdivia HH and Delmar M. Plakophilin-2 is required for transcription of genes that control calcium cycling and cardiac rhythm. *Nature communications*. 2017;8:106.
3. Lubkemeier I, Requardt RP, Lin X, Sasse P, Andrie R, Schrickel JW, Chkourko H, Bukauskas FF, Kim JS, Frank M, Malan D, Zhang J, Wirth A, Dobrowolski R, Mohler PJ, Offermanns S, Fleischmann BK, Delmar M and Willecke K. Deletion of the last five C-terminal amino acid residues of connexin43 leads to lethal ventricular arrhythmias in mice without affecting coupling via gap junction channels. *Basic Res Cardiol*. 2013;108:348.
4. Takefuji M, Wirth A, Lukasova M, Takefuji S, Boettger T, Braun T, Althoff T, Offermanns S and Wettschureck N. G(13)-mediated signaling pathway is required for pressure overload-induced cardiac remodeling and heart failure. *Circulation*. 2012;126:1972-1982.
5. Dobin A, Davis CA, Schlesinger F, Drenkow J, Zaleski C, Jha S, Batut P, Chaisson M and Gingeras TR. STAR: ultrafast universal RNA-seq aligner. *Bioinformatics*. 2013;29:15-21.
6. Ringner M. What is principal component analysis? *Nat Biotechnol*. 2008;26:303-304.
7. Lohr C. Monitoring neuronal calcium signalling using a new method for ratiometric confocal calcium imaging. *Cell Calcium*. 2003;34:295-303.
8. Grynkiewicz G, Poenie M and Tsien RY. A new generation of Ca<sup>2+</sup> indicators with greatly improved fluorescence properties. *J Biol Chem*. 1985;260:3440-3450.
9. Lipp P, Huser J, Pott L and Niggli E. Subcellular properties of triggered Ca<sup>2+</sup> waves in isolated citrate-loaded guinea-pig atrial myocytes characterized by ratiometric confocal microscopy. *J Physiol*. 1996;497 ( Pt 3):599-610.
10. Nilbratt M, Porras O, Marutle A, Hovatta O and Nordberg A. Neurotrophic factors promote cholinergic differentiation in human embryonic stem cell-derived neurons. *J Cell Mol Med*. 2010;14:1476-1484.
11. Trollinger DR, Cascio WE and Lemasters JJ. Selective loading of Rhod 2 into mitochondria shows mitochondrial Ca<sup>2+</sup> transients during the contractile cycle in adult rabbit cardiac myocytes. *Biochemical and biophysical research communications*. 1997;236:738-742.
12. Lundby A, Rossin EJ, Steffensen AB, Acha MR, Newton-Cheh C, Pfeufer A, Lynch SN, Consortium QTIIG, Olesen SP, Brunak S, Ellinor PT, Jukema JW, Trompet S, Ford I, Macfarlane PW, Krijthe BP, Hofman A, Uitterlinden AG, Stricker BH, Nathoe HM, Spiering W, Daly MJ, Asselbergs FW, van der Harst P, Milan DJ, de Bakker PI, Lage K and Olsen JV. Annotation of loci from genome-wide association studies using tissue-specific quantitative interaction proteomics. *Nat Methods*. 2014;11:868-874.
13. Lundby A and Olsen JV. GeLCMS for in-depth protein characterization and advanced analysis of proteomes. *Methods Mol Biol*. 2011;753:143-155.
14. Alvarado FJ, Chen X and Valdivia HH. Ablation of the cardiac ryanodine receptor phospho-site Ser2808 does not alter the adrenergic response or the progression to heart failure in mice. Elimination of the genetic background as critical variable. *J Mol Cell Cardiol*. 2017;103:40-47.
15. Tonzi P, Yin Y, Lee CWT, Rothenberg E and Huang TT. Translesion polymerase kappa-dependent DNA synthesis underlies replication fork recovery. *Elife*. 2018;7:e41426.



16. Huang F, Hartwich TM, Rivera-Molina FE, Lin Y, Duim WC, Long JJ, Uchil PD, Myers JR, Baird MA, Mothes W, Davidson MW, Toomre D and Bewersdorf J. Video-rate nanoscopy using sCMOS camera-specific single-molecule localization algorithms. *Nat Methods*. 2013;10:653-658.
17. van der Walt S, Schonberger JL, Nunez-Iglesias J, Boulogne F, Warner JD, Yager N, Gouillart E, Yu T and scikit-image c. scikit-image: image processing in Python. *PeerJ*. 2014;2:e453.
18. Ester M, Kriegel H-P, Sander JD and Xu X. *Proceedings of the Second International Conference on Knowledge Discovery and Data Mining (KDD-96)* Portland, OR: AAAI Press; 1996.
19. Kondo RP, Wang SY, John SA, Weiss JN and Goldhaber JL. Metabolic inhibition activates a non-selective current through connexin hemichannels in isolated ventricular myocytes. *J Mol Cell Cardiol*. 2000;32:1859-1872.
20. Li H, Liu TF, Lazrak A, Peracchia C, Goldberg GS, Lampe PD and Johnson RG. Properties and regulation of gap junctional hemichannels in the plasma membranes of cultured cells. *J Cell Biol*. 1996;134:1019-1030.
21. Beuckelmann DJ and Wier WG. Sodium-calcium exchange in guinea-pig cardiac cells: exchange current and changes in intracellular Ca<sup>2+</sup>. *J Physiol*. 1989;414:499-520.
22. Vanslebrouck B, Kremer A, Pavie B, van Roy F, Lippens S and van Hengel J. Three-dimensional reconstruction of the intercalated disc including the intercellular junctions by applying volume scanning electron microscopy. *Histochem Cell Biol*. 2018;149:479-490.
23. Gutstein DE, Morley GE, Tamaddon H, Vaidya D, Schneider MD, Chen J, Chien KR, Stuhlmann H and Fishman GI. Conduction slowing and sudden arrhythmic death in mice with cardiac-restricted inactivation of connexin43. *Circ Res*. 2001;88:333-339.
24. Morley GE, Danik SB, Bernstein S, Sun Y, Rosner G, Gutstein DE and Fishman GI. Reduced intercellular coupling leads to paradoxical propagation across the Purkinje-ventricular junction and aberrant myocardial activation. *Proc Natl Acad Sci U S A*. 2005;102:4126-4129.
25. Morley GE, Vaidya D and Jalife J. Characterization of conduction in the ventricles of normal and heterozygous Cx43 knockout mice using optical mapping. *J Cardiovasc Electrophysiol*. 2000;11:375-377.
26. Vaidya D, Morley GE, Samie FH and Jalife J. Reentry and fibrillation in the mouse heart. A challenge to the critical mass hypothesis. *Circ Res*. 1999;85:174-181.
27. Sikkel MB, Francis DP, Howard J, Gordon F, Rowlands C, Peters NS, Lyon AR, Harding SE and MacLeod KT. Hierarchical statistical techniques are necessary to draw reliable conclusions from analysis of isolated cardiomyocyte studies. *Cardiovasc Res*. 2017;113:1743-1752.
28. Camors E and Valdivia HH. CaMKII regulation of cardiac ryanodine receptors and inositol triphosphate receptors. *Front Pharmacol*. 2014;5:101.